DYNAMIC CHARACTERISTICS AND MODAL PARAMETERS OF A PLATE WITH A SURFACE CRACK

YIN CHEN

Dynamic Characteristics and Modal Parameters Of a Plate With a Surface Crack

by

© Yin Chen, B.Eng., M.Eng.

A thesis submitted to the School of Graduate Studies

in partial fulfillment of the requirements for the degree of

Master of Engineering

Faculty of Engineering and Applied Science

Memorial University of Newfoundland

December, 1992

St. John's Newfoundland Canada

ISBN 0-315-82641-X

Canada

Abstract

A systematic study of the behaviour of a plate with a surface crack is carried out using the finite element method. Static, steady state, resonant and transient responses of the cracked plate are examined. Strain, displacement and acceleration responses without/with the crack are computed. Modal analysis is performed to determine the natural frequencies, mode shapes and strain/displacement frequency response functions. Frequency response functions without/with the crack are computed. Strain mode shapes, as well as displacement mode shapes, are obtained. The difference of the strain mode shapes between the uncracked plate and the cracked plate is calculated. Each of the parameters mentioned above is examined to determine the sensitivity of this parameter to the crack that occurs in the structure.

By using all the methods of analysis mentioned above, and comparing the sensitivity of different parameters to cracking, it is found that the surface crack in the structure will affect most of the dynamic characteristics such as strain/stress field around the crack, natural frequencies of the structure, amplitudes of the response and mode shapes. Some of the most sensitive parameters are the difference of the strain mode shapes and the local strain frequency response functions. By monitoring the changes in the local strain frequency response functions and difference of strain

mode shapes, the location and severity of the crack that occurs in the structure can be determined. Based on these results, suitable procedures for detecting the crack in real structures are suggested.

Acknowledgements

First of all, I would like to thank Dr. A.S.J. Swamidas, my supervisor. His supervision and financial assistance are graciously acknowledged. The financial support from Faculty of Engineering and Applied and the School of Graduate Studies is also greatly appreciated.

I would also like to extend my gratitude to my friends Mr. Jing Xiao and Mr. Bin Zou, for their help in using the ABAQUS and the Latex, and for the many useful discussions with them.

Contents

List of Figures

List of Tables

Nomenclature

$[M]$	mass matrix
$[K]$	stiffness matrix
$[C]$	damping matrix
$\{F\}$	force vector
$[U]$	modal matrix
$[m]_{modal}$	diagonal modal mass matrix
$[k]_{modal}$	diagonal modal stiffness matrix
$[c]_{modal}$	diagonal modal damping matrix
ω_i	ith natural frequency
ϕ_i	ith displacement mode shape
ϵ_N	Nth member deformation
ϵ	strain
u	displacement
ϵ_r	modal strain for rth mode

$S_{jk,\epsilon}(\omega)$	strain frequency response function
$[G], [H]$	system matrix
$[H^{\epsilon}]$	force-strain transfer function
$[\Lambda]$	force-displacement transfer function
$[\psi^{\epsilon}]$	strain mode shape matrix
E	Young's modulus
μ	poisson's ratio
ρ	mass density
N	shape functions
$\{a^{e}\}$	nodal displacement
σ	stress
D	elasticity matrix
r	external concentrated nodal forces
ϕ	rotation of the plate
TH	thickness of the plate
d	depth of the surface crack
L	Laplace transform operator
s	Laplace variable
ω	Fourier variable

H	transfer function
s_i	ith eigenvalue

Chapter 1

Introduction

Structures under repeated regular/irregular loadings inevitably develop cracks. For instance, offshore structures are subjected to repeated loadings due to ocean waves which impose a large number of cyclic stresses; under these varying cyclic stresses fatigue cracks develop at critical welded junctions of offshore structures. Therefore the prediction, detection and monitoring of cracks in structures have been the subject of intensive investigations during recent years. Its importance is shown in the strict guidelines enforced on the design of structures and structural components, as well as on the maintenance and repair carried out on in-situ structures for maximum effectiveness at minimum cost. Many theoretical and experimental studies of the behaviour of structures with cracks have been carried out to develop a feasible methodology. Thousands of theoretical and experimental studies have been carried

out in the allied area of fracture mechanics. Meanwhile, many techniques have been developed to quantify cracking in structures, such as acoustic emission, magnetic particle inspection, alternating/direct current field measurement, eddy current, ultrasonics and modal testing.

In recent years, Non-Destructive Evaluation (NDE) has gained a greater attention for monitoring and detecting cracks developed in operating structures, and several techniques have been developed, as mentioned before. Each of these methods has its own advantages and disadvantages. New techniques are being developed to meet the new requirement of structures in more and more severe environments. Among these newly emerging techniques, the procedure for modal analysis and testing is being explored by many researchers to determine whether it can be used as an efficient technique, especially if the modal strains around the critical zones could be monitored. Earlier studies on modal analysis proved to be ineffective since the researchers considered only the frequency shifts and these shifts could be caused by a number of factors such as cracking and damage, erosion and strength degradation of the foundation, addition of extraneous mass to the sub/super structure, etc. Recent studies in modal analysis has been focussed on the total dynamic behaviour.

The physical properties of any structure can be expressed in term of its mass, stiffness and damping. Any damage that occurs in the structure will cause changes in theses physical properties; and these changes will be reflected in the change of the

dynamic characteristics of the structure, such as natural frequencies, mode shapes, displacements, strains/stresses, and damping. This study investigates the sensitivities of the dynamic characteristics of any structure to crack development so as to develop a new technique to monitor and detect cracks or damages in structures, especially in offshore/onshore structures. As an initial study in this area of crack detection and prediction for small cracks using modal analysis, the scope of this study is to determine the change in the dynamic characteristics and modal parameters of a plate with a surface crack. How do these parameters change as the depth of the crack increases? Different modes of response have been examined to relate the global and local changes shown as a consequence of cracking. Static, steady state, resonant and transient (dynamic) responses have been considered as a small crack increases in depth due to stress cycling. Greater emphasis has been laid on the examination of strain frequency response functions (FRFs) and strain modal shapes, which are independent to the amplitude of applied forces, and give a better and more sensitive indication of the location and severity of the crack.

The subject matter of the above study is developed further in this thesis as mentioned below, viz.,

1. Literature review of earlier studies on damage detection, and the latest methodology of examining the modal strain development are given in Chapter 2.

2. The static analysis of the structure using finite element analysis is detailed in Chapter 3. Strain, displacement and rotation developed around a location, wherein the possibility for cracking exists, is investigated in detail for the case of a structure without/with the crack to determine the limits of changes that could occur in these parameters.

3. The fourth chapter deals with the steady state analysis of a structure without/with a crack. Frequency response functions of surface strains near the crack, and the acceleration and displacement frequency response functions away from the crack are computed and compared as the crack grows through the thickness.

4. The resonant and the transient response analyses are detailed in Chapter 5 to outline the modal information that could be obtained from these investigations to identify and localize cracking zones and extent of cracking. Power spectral response is also analyzed to determine the changes that occur due to cracking.

5. The salient conclusions from the above studies are summarized in Chapter 6 and possible areas for further detailed investigation are also outlined.

Chapter 2

Literature Review

2.1 Nondestructive Evaluation and Damage Detection by Modal Analysis

The detection of cracks in components of structures in service is very essential and important to ensure the integrity of structures since these cracks tend to propagate and cause sudden failures which are usually very costly in terms of human life and property damage. Therefore nondestructive evaluation (NDE) techniques are widely used for damage detection. Some of the well-known techniques are acoustic emission, magnetic particle inspection, alternating/direct current field measurement, eddy current and ultrasonics. Each of these tech-

niques has its own advantages and disadvantages. As pointed out by Gomes el al. (1990) the use of most of the well known NDE techniques may be inconvenient in many situations due to the need for the investigator to have access to the component under operating conditions. Therefore a new NDE technique using the vibrational characteristics of structures via modal analysis has been recently considered by many researchers.

Shahrivar et al. (1986) determined the natural frequency shifts in an offshore structure due to the presence of damages in structural elements. Modal testing of an offshore framed platform model, with grossly cracked structural members (severed members), was performed and a reduction in natural frequencies and increase in structural responses were reported.

Springer et al. (1990) reported that a boxbeam structure was built and tested at the Marshall Space Flight Center (MSFC) for the purpose of evaluating the ability of the modal test to detect the presence of structural faults in space flight hardware. A finite element model of this structure was also developed and used to simulate the modal test results. The results of finite element analysis compared favourably with the test data. No further results were presented in the paper.

Gomes and Silva (1990, 1991 and 1992) conducted a series of studies using

modal analysis for crack identification in simple structures. Modal tests of cantilever beams with fatigue cracks at different locations for different crack depths were performed. The influence of a lumped mass, which was attached to the structure (to simulate the end loads in structures), was also studied. The main modal parameters that were monitored were the natural frequencies of the vibrating beam. A series of nondimensional curves and tables depicting the changes in natural frequencies for various depths of the crack, location of the crack, and the lumped mass were presented. Use of these tables and figures would lead to the identification of the probable depth and location of the crack in any cantilever beam.

Richardson and Mannen (1991) developed modal sensitivity functions for the location of structural faults due to a change of mass, stiffness and/or damping of structural components. Equations of motion considering modes of vibration and structural response were given by:

$$[M]\{\ddot{X}(t)\} + [C]\{\dot{X}(t)\} + [K]\{X(t)\} = \{F(t)\} \tag{2.1}$$

where [M] is the mass matrix; [K] is the stiffness matrix; and [C] is the damping matrix.

For a lightly damped structure, the following orthogonality conditions are

valid:

$$[U]^T[M][U] = [m]_{modal} \tag{2.2}$$

$$[U]^T[C][U] = [c]_{modal} \tag{2.3}$$

$$[U]^T[K][U] = [k]_{modal} \tag{2.4}$$

where $[m]_{modal}$ is the diagonal modal mass matrix; $[k]_{modal}$ is the diagonal modal stiffness matrix; $[c]_{modal}$ is the diagonal modal damping matrix, and [U] is the modal displacement matrix.

Two other relationships which result from the orthogonality conditions are:

$$\Omega_{0_k}^2 = \frac{k_k}{m_k} \tag{2.5}$$

$$2d_{0_k} = \frac{c_k}{m_k} \tag{2.6}$$

where: $\Omega_{0_k}^2 = \omega_{0_k}^2 + d_{0_k}^2$

and: $\omega_{0_k}^2, d_{0_k}^2$ = frequency and damping of the uncracked structure.

If only stiffness changes occur in the structure due to cracking, then Eqns. (2.4), (2.5) and (2.6) become:

$$[U + dU]^T[K + dK][U + dU] = [k + dk]_{modal} \tag{2.7}$$

$$\Omega_{1_k}^2 = \frac{k_k + dk_k}{m_k} \tag{2.8}$$

$$2d_{1_k} = \frac{c_k}{m_k} \tag{2.9}$$

where: $\Omega_{1k}^2 = \omega_{1k}^2 + d_{1k}^2$

and: ω_{1k}^2, d_{1k}^2 = frequency and damping of the cracked structure.

Scaling the mode shapes to get unity modal masses so that $m_k = 1$ for all modes (k), and subtracting Eqn. (2.4) from Eqn. (2.7), the stiffness sensitivity equation can be obtained as:

$$\{U_k + dU_k\}^T[dK]\{U_k+dU_k\}+2\{dU_k\}^T[K]\{U_k\}+\{dU_k\}^T[K]\{dU_k\} = {\omega_{1k}}^2-{\omega_{0k}}^2 \tag{2.10}$$

For small stiffness changes, where the fault is small enough so that the mode shapes don't change substantially (i.e., $dU_k = 0$), the stiffness sensitivity equation given in Eqn. (2.10) is simplified as:

$$\{U_k\}^T[dK]\{U_k\} = {\omega_{1k}}^2 - {\omega_{0k}}^2 \tag{2.11}$$

Using Eqn. (2.10) or (2.11), when the change in natural frequency of kth mode is known, the corresponding change in stiffness can be obtained, and vice-versa. Normally cracks in the structure tend to reduce the stiffness of the structure. From Eqn. (2.10), a natural frequency reduction is predicted. For mass and damping changes, similar sensitivity equations were derived in their paper.

Stubbs et al. (1990) also derived expressions for changes in modal stiffness in terms of modal masses, modal damping, eigenfrequencies, eigenvectors, and

their respective changes.

Most researchers have stated that damages in structures tend to reduce the natural frequencies; consequently knowing the changes in natural frequencies it is possible to determine the extent of cracks or damages in a structure. But it is hard to determine the location of the crack by this procedure since cracks at two different locations, associated with certain crack lengths or depths, may cause the same amount of frequency shift at certain modes. However Hearn et al. (1991) have pointed out in their paper that the magnitudes of changes for different natural frequencies is a function of the severity and the location of flaws in the structure. Therefore ratios of changes in natural frequencies, normalized with respect to the largest frequency change, are independent of severity for small flaws and can serve to indicate the location of flaws directly. The theory was based on the concept that a single crack will affect each vibration mode differently, having a strong affect on certain modes and a weak effect on others. This dissimilarity of effect on various modes, since it can be predicted, is the basis for the identification of damaged members. The procedure was stated as follows: Natural vibration frequencies are to be measured periodically. When changes in natural frequencies are observed, the set of ratios of changes are computed and compared with the various member

characteristic ratio ensembles obtained from the equation:

$$\frac{\Delta\omega_i^2}{\Delta\omega_j^2} = \frac{\frac{\epsilon_N{}^T(\phi_i)k_N\epsilon_N(\phi_i)}{\Phi_i{}^T M\Phi_i}}{\frac{\epsilon_N{}^T(\phi_j)k_N\epsilon_N(\phi_j)}{\Phi_j{}^T M\Phi_j}} \tag{2.12}$$

where $\Delta\omega_i$ and $\Delta\omega_j$ are the changes of the natural frequency of ith mode and jth mode, respectively, due to cracking. ϵ_N are the Nth member deformations and have the following relationship with displacement mode shape and stiffness of the whole structure:

$$\phi_i^T K \phi_i = \sum \epsilon_N{}^T(\phi_i) k_N \epsilon_N(\phi_i) \tag{2.13}$$

where ϕ_i is the ith displacement mode shape; M is the mass of the structure; K is the stiffness of the whole structure; and k_N is the stiffness of Nth member. The location of the crack is determined by selecting the member characteristic ensemble that most closely match the observed ratios of frequency changes. This method can identify the location of cracked members of the structure.

Pandy el al. (1991) used changes in curvature mode shapes to determine the location of the damage. They examined a cantilever beam and a simply supported beam. Instead of displacement mode shapes, curvature mode shapes were calculated. Absolute differences between the curvature mode shapes for the intact and the damaged beam were calculated. The largest differences occurred at the damaged point. Therefore they stated that absolute differences

of the curvature mode shapes between the intact and the damaged structures could serve to indicate the location of damage in the structure.

Recently a study concerning both the severity and location of the crack in offshore structures was carried out by Swamidas and Chen (1992). They used strain gauges in the modal testing, monitoring both the global and local changes in frequency and amplitude of strain frequency response functions. Also they carried out a finite element analysis for the modal response of the structure and determined the frequency response functions for displacements and accelerations. The results showed that local surface strain frequency response functions were very sensitive to the presence of cracking in the structure and was strongly recommended for the detection of cracking in structures.

2.2 Strain Modal Testing

As pointed out in the previous paragraph, modal strains are very sensitive to local damage. Chen and Swamidas (1992) conducted an experiment which showed that the amplitude of the strain frequency response function near the crack zone decreased considerably when the crack size increased. They reported that in the main column of a tripod tower platform model, with a diameter of 300 mm and a thickness of 3 mm, the amplitude of the local

strain FRF at the first resonant frequency decreased by more than 60 % when the crack became a through crack, with a length of 90 mm (45° inclination). They used accelerometers, linear variable displacement transducers (LVDT), and strain gauges in their experiment. They proposed a procedure to detect cracks in offshore structures: from the global sensors such as accelerometers determine the natural frequency changes that occur in the structure. When there is a change in the natural frequencies of the structure, there is a possibility that a crack has started to grow in the structure. Then monitor the local sensors (strain gauges applied in the critical areas of the structure) to find out the location and magnitude of the crack.

O. Bernasconi and D.J. Ewins (1989) have examined in detail the behaviour of modal strain/stress fields. They defined "modal strain" from the general theory of solid elastodynamics. It is assumed that any displacement field for the body may be expanded as a convergent series of mode shapes:

$$u = \sum C_r \phi_r \tag{2.14}$$

where $C_r = \int_V M u \phi_r dV$ and ϕ_r is the rth mode shape.

For small displacements, the strain field can be defined as:

$$\epsilon = Du = \sum C_r D(\phi_r) \tag{2.15}$$

where D is a linear differential operator.

The modal strain can then be defined as

$$\epsilon_r = D(\phi_r) \tag{2.16}$$

Using this definition, the strain frequency response function is derived as:

$$S_{jk}(\omega) = \sum \phi_r^k \epsilon_r^j / (\overline{\omega}_r{}^2 - \omega^2) \tag{2.17}$$

where k is the excitation point and j is the response point.

Later on, they used this theory and applied the strain modal testing on real structures which included: (i) a discontinuous cantilever beam, (ii) a curved plate, and (iii) a steam turbine blade. The conclusion they reached in their study was that the mass-normalized modal strains could be either computed using finite element method, or measured using strain gauges.

Tsang (1990) proposed a governing equation for strain response function which was obtained in a manner similar to that used for determining a set of structural system matrices from experimental inertance measurements on a vibrating structure. Using a form similar to the displacement response function, viz.,

$$(-\omega^2[M] + [K])\{U(\omega)\} = \{f(\omega)\} \tag{2.18}$$

he proposed using the following form:

$$(-\omega^2[G] + [H])\{\epsilon(\omega)\} = \{f(\omega)\} \tag{2.19}$$

where [M] and [K] are mass and stiffness matrices, respectively, [G] and [H] are defined as system matrices for strain which did not have any physical interpretation yet, $\epsilon(\omega)$ is the strain response function and $f(\omega)$ is the forcing function used in the investigation. The proposed methodology was verified using finite element analysis theory and an algorithm to formulate the system matrices [G] and [H] from experimental strain data was derived.

Li et al. (1989) also derived an expression for the strain transfer function. Their derivation was also from the vibration equation which was the same as Eqn. (2.1). Then based on the relationships between strain and displacement, a theoretical expression for the strain response was derived. For one dimensional problems, it has the form as follows:

$$\{\epsilon\} = [\psi^{\epsilon}][\Lambda]^{-1}[\phi]\{F\} = [H^{\epsilon}]\{F\} \tag{2.20}$$

where $[H^{\epsilon}]$ is the force-strain transfer matrix or strain transfer function; $[\phi]$ the displacement mode shape matrix, $[\psi^{\epsilon}]$ the strain mode shape matrix, and $[\Lambda]$ the transfer function matrix for displacements. Using this theory, they obtained the strain transfer function of a plate and a beam from the strain gauge readings. Consecutively, they identified the modal parameters and the displacement and the strain mode shapes. The displacement mode shape obtained by the strain transfer function was compared with the displacement

mode shape obtained by using the accelerometers, and a good match was found.

In the study cited earlier Pandy et al. (1991) had used changes in curvature mode shapes to determine the location of the damage; since the curvature is proportional to the surface strain, the strain mode shape would as well give a similar information on the damage that occurs in the structure.

2.3 Miscellaneous

Besides the literature reviewed above, many other researchers have carried out studies on the behaviour of structure with cracks. Collins et al. (1992) studied the free and forced longitudinal vibrations of a cantilever bar with a crack, and the effect of the crack location and compliance on the fundamental natural frequencies was determined. Rajab et al. (1991) examined the vibrational characteristics of cracked shafts, derived relationships between the crack depth and location on the shaft to changes in the first few natural frequencies. Collins et al. (1991) reported the response of a rotating Timoshenko shaft with a single transverse crack under axial impulses. The relationships between the maximum displacement and the crack depth was presented. Chondros et al. (1989) studied the change in the natural frequencies and modes of vibration of

the structure with a given geometry of a crack. Earlier Chondros et al. (1980) had investigated the relationships between the change in natural frequency of vibration of a cantilever beam and the crack depth that occurred at the welded junctions. Besides these many other researchers have carried out studies on frequency changes that occur in structures using conventional vibration studies. Most of these studies considered only the frequency shifts that occur due to the existence and growth in crack depth and width; and most of these studies were on gross cracking in members such as severing of members, etc.

2.4 Summary

Earlier studies which have been reviewed above have investigated the behaviour of cracked structures in a global sense. Most of these studies have examined the change in natural frequencies of the cracked structure. Some have studied the change in the curvature mode shapes and the maximum displacement. The size of the crack considered in these studies is relatively large. The use of strain modal analysis and testing, for the detection of cracks in the structure, is a relatively new concept and very few studies have been reported so far using this technique. The study presented in this thesis is focused on a small crack and the consequent changes that occur in the structural re-

sponse. Besides the natural frequencies, displacements, modal displacement amplitudes and displacement mode shapes which have been examined in the earlier studies, other parameters such as strain amplitudes, modal strains and strain mode shapes are examined. Local parameters, as well as global parameters, have been examined to monitor the changes that occur during the growth in crack depth.

Chapter 3

Static Analysis of a Plate with a Surface Crack

3.1 Finite Element Modelling

In order to have a better understanding of the behaviour of structures with surface cracks, a finite element model of a simple cantilever plate, with a surface crack, was investigated in this thesis; the plate was fixed at one end, and free at all other three edges. Fig. 3.1 shows the geometric dimension of the plate and the location of the surface crack. The choice of this boundary condition was to satisfy the requirements for an experimental investigation

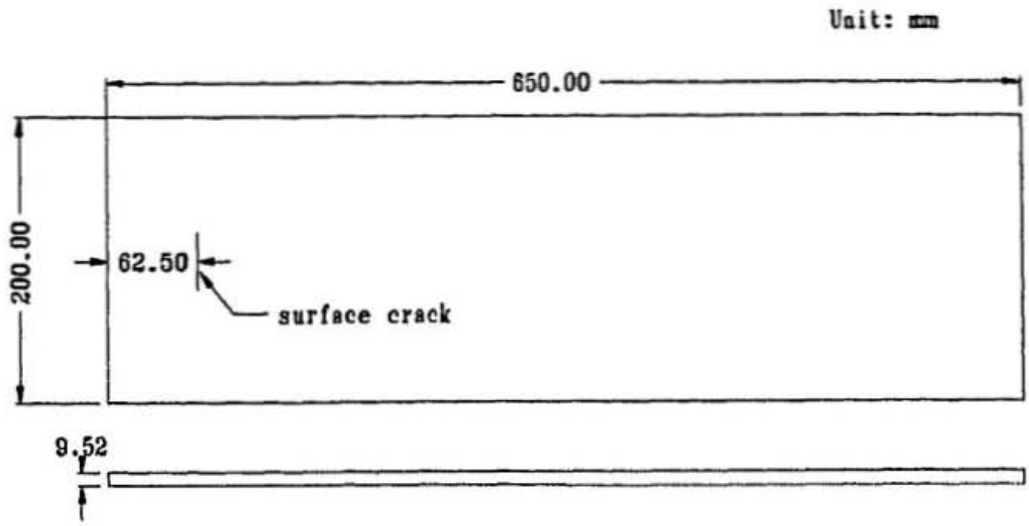

Figure 3.1: Geometric dimensions of the plate

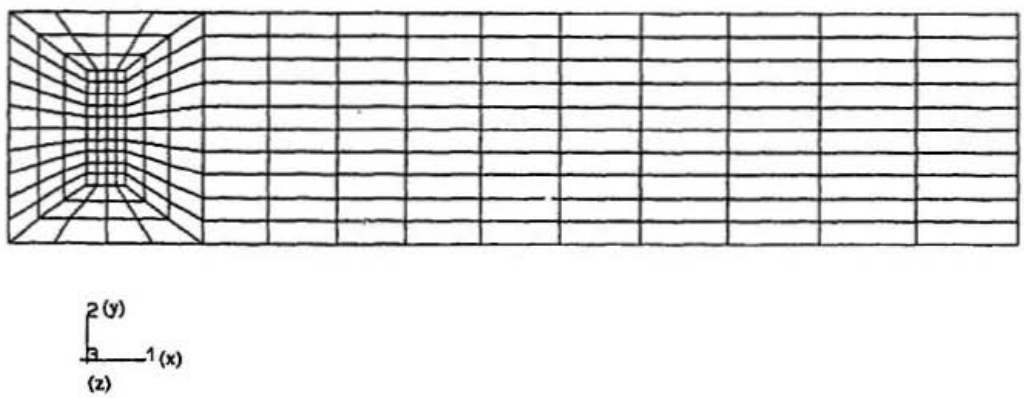

Figure 3.2: Finite element mesh of the plate

which will be carried out in the near future on a similar plate. The material of the plate is steel with a thickness of 9.525 mm, Young's modulus $E = 207 \times 10^9 N/m^2$, mass density $\rho = 7860 kg/m^3$, and Poisson's ratio $\mu = 0.29$. The coordinate system is shown in Fig. 3.2, with the x-axis along the long side of the plate, and the y-axis along the short side. The finite element mesh is also shown in Fig. 3.2. In order to get better results around the crack, a finer mesh was introduced around the crack area. The general purpose finite element computer software ABAQUS was used to carry out the finite element analysis. Quadrilateral shell elements with 8 nodes and a 2×2 reduced integration, and 6 nodes line spring elements were used. The surface crack was simulated by the line spring elements. In this part of the study, the cantilever plate is analyzed for its static response to identify patterns for nondestructive evaluation.

3.1.1 Basic Finite Element Equations

In finite element analysis, the displacement at any point is given by:

$$u \simeq \hat{u} = \sum N_i a_i = N a^e \tag{3.1}$$

where N, the shape function matrix, is dependent on the position of the node in the xy-plane and a^e is a list of nodal displacements.

With displacements known at all points the strain at any point can be determined as:

$$\epsilon = Su \simeq \sum B_i a_i = Ba^e \tag{3.2}$$

$$B_i = SN_i \tag{3.3}$$

also,

$$B = SN \tag{3.4}$$

where S is a suitable linear operator.

Then for the general linear elastic behaviour, the stresses can be determined as:

$$\sigma = D(\epsilon - \epsilon_0) + \sigma_0 \tag{3.5}$$

where D is an elasticity matrix containing the appropriate material properties; ϵ_0 is the initial strain and σ_0 is the initial stress.

From the principle of virtual displacements, the following approximate equilibrium equations can be obtained:

$$Ka + f = r \tag{3.6}$$

$$K_{ij} = \int_V B_i^T D B_j dV \tag{3.7}$$

where K is the stiffness matrix; r is the external concentrated nodal forces; and f represents forces due to body forces, surface forces, initial strain, and initial stress (Zienkiewicz and Taylor, 1989).

3.1.2 Shell Element

The element type used in this study is S8R, with 8 nodes; it is a doubly curved shell element. It has a 3×3 middle surface integration for mass, body forces and surface pressure calculation and a 2×2 integration for constitutive calculation and output. Five integration points are chosen through the shell thickness. They are located from the bottom to the top surface of the shell, with equal distances between two adjacent points (Hibbitt et al.'s ABAQUS manuals, 1989). The strain and stress could be output at any of these five points through the shell thickness. In this study, surface strains are focused on to compare the measurements from strain gauges. Therefore, only the surface strain values are chosen for the output.

For displacement output, S8R type shell element of ABAQUS can only output nodal displacements at the reference surface, which is the middle of the shell section (if the thickness is equal throughout the whole model, which is the situation for the problem considered in this study). But in practical measurements, it is impossible to measure the displacements at the middle surface. Since this study is trying to develop a technique to detect cracking in structures, and under practical situations, only surface displacements could be measured, only the surface displacements should be calculated and output.

The ABAQUS shell element formulation is based on the Kirchhoff constraint assumptions of the "thin" shell theory. The constraints require a material line, that is originally normal to the shell's reference surface, to remain normal to that surface throughout the deformation state. So the surface displacement is equal to the displacement at reference surface plus the corresponding rotation multiplied by the thickness of the shell section.

$$u_{sur} = u_{ref} + \phi \times TH/2 \tag{3.8}$$

where u_{sur} is the displacement at the surface of the plate, u_{ref} is the displacement at the reference surface, ϕ is the rotation at the reference surface, and TH is the thickness of the plate.

When the displacement at reference surface is very small (it is equal to zero in pure bending) in comparison to the rotation times the thickness of the plate, then the first term on the right hand side of the Eqn. (3.8) can be ignored. The surface displacement can be calculated by:

$$u_{sur} \simeq \phi \times TH/2 \tag{3.9}$$

3.1.3 Line Spring Element

Line spring elements provide a computationally inexpensive tool for the modelling of surface cracks in plates and shells. The basic concept was first pro-

posed by Rice (1972) and has been further discussed by Parks and White (1982). The "line spring" is a series of one-dimensional finite elements placed along the part-through flaw, which allows local flexibility of one side of the flaw with respect to the other (point A and B in Fig. 3.3.). This local flexibility is calculated from existing solutions for single edge notch specimens under plane strain conditions (by means of fracture mechanics) (Fig. 3.4). The whole approach is computationally inexpensive in comparison to full three-dimensional models of the vicinity of the flaw. It is also pointed out in the ABAQUS manual that the practical experience with this method on typical geometries has shown that, for several important geometries, the method provides acceptable accuracy. The major approximation occurs in the vicinity of the flaw as it penetrates a surface, if the results are compared with the results of a full three-dimensional model. Since this study was to develop a practical method to detect cracking in structures, and in the actual application, it is impossible to apply sensors (strain gauges) very close to the crack, therefore the output values which are not in the vicinity of the crack, would be better represented by results from the model using the line spring elements. The geometric profile of the surface crack is taken to be a semi-elliptical one, as shown in Fig. 3.5.

In this study, the depth of the crack means the maximum crack depth in the

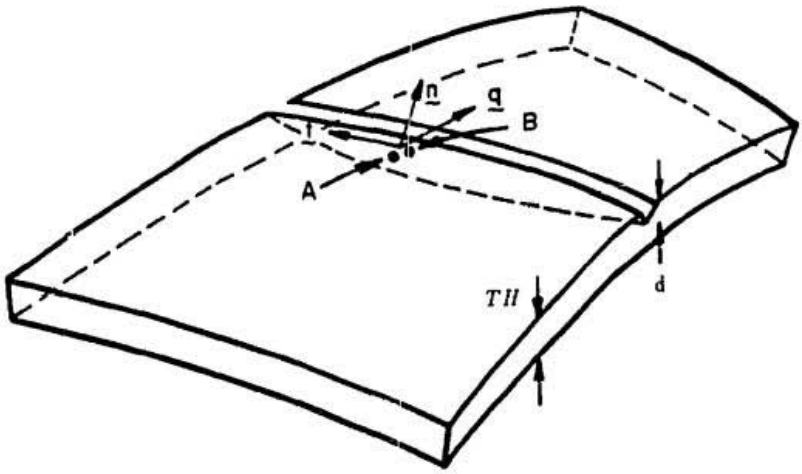

Figure 3.3: Line spring modelling

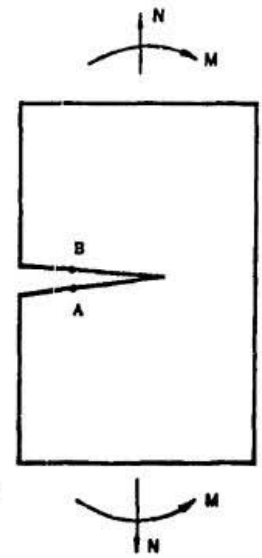

Figure 3.4: Line spring compliance calibration model

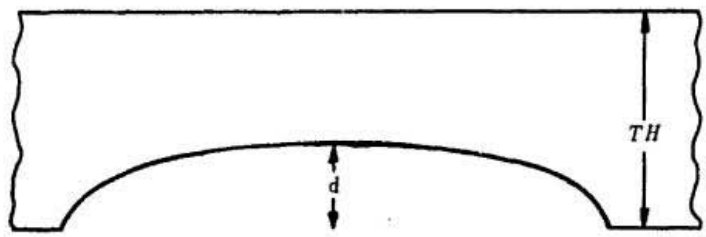

Figure 3.5: Geometric profile of the surface crack

middle of the crack. The surface length of the crack to be sensed is taken as 40 mm. The depth of the crack varies from zero to 6.667 mm (70% of the thickness of the plate). The increment of the change of the crack depth is taken as 5% of the thickness.

3.2 Analysis and Results

3.2.1 Surface Strain/Stress

A concentrated vertical load was applied at the centre of the free end of the plate. The location of the crack, as could be noted from Figs. 3.1 and 3.2, is close to the fixed end. Therefore, the concentrated load will not have a local effect on the strain/stress field around the crack. In the following discussions the cracked plate means that the plate has a maximum crack depth of 6.667 mm and a surface crack length of 10 mm. The applied load was 500 N.

Figs. 3.6 and 3.7 show the contours of the normal stress σ_x of the plate without/with the surface crack. A heavy stress concentration is observed around the two ends of the crack; while away from the crack, there is almost no difference for the stress of the plate with and without the crack. It shows that the use of line spring elements for simulating a surface crack is successful in showing the actual stress variation around the crack zone.

In this study, a major concern is the nature of surface strains which could be measured by strain gauges in the real structure. Since the concentrated load is applied vertically at the free end, the bending stresses/strains σ_x/ϵ_x are dominant. The largest values of the stresses/strains occur along the x-axis.

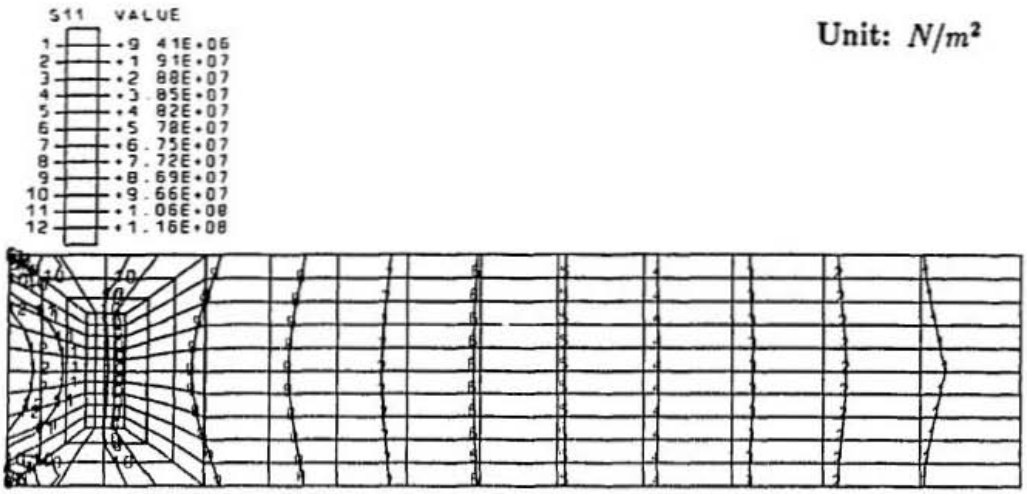

Figure 3.6: Contours of the normal stress σ_x without a surface crack

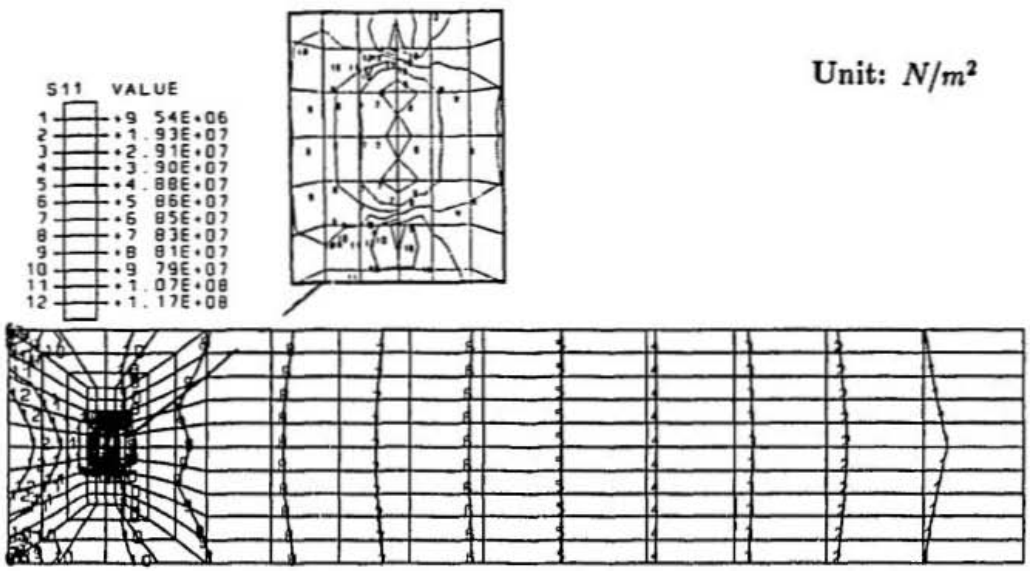

Figure 3.7: Contours of the normal stress σ_x with a surface crack

Consequently ϵ_x, at the surface of the plate, is calculated and compared.

Fig. 3.8 shows the contours of the surface strain ϵ_x without the surface crack, and Fig. 3.9 shows the contours of the same strain component with the surface crack. The crack depth is 6.667 mm, which is 70% of the thickness of the plate. It can be observed that at the tip of the crack there are heavy strain concentration areas; while at the middle of the crack there are some strain release areas. It is also noticed that with this crack size and depth, a large portion of area around the crack are affected; hence a strain gauge, located at a suitable distance (around 16 mm) away from the crack will be able to sense the presence of the crack showing a change of 8.8% in strain (see Table 3.1). Fig. 3.10 shows the decrease of the normalized strain level as the depth of the surface crack increases. The measurement points are 1.6 mm, 7.8 mm and 15.8 mm away from the crack. It is observed that when the crack depth is equal to 70% of the thickness of the plate, the strain level decreases are around 37.4%, 20.9% and 8.8% for the measurement points 1.6mm, 7.8 mm and 15.8 mm away from the crack, respectively. This shows that even when a crack is small, it is possible to identify the crack in the structure using static measurements. It must be emphasized here that the strain gauge must be located around the shadow region of the crack to sense an appreciable level of strain changes due to crack growth. It should also be pointed out that the static measurements

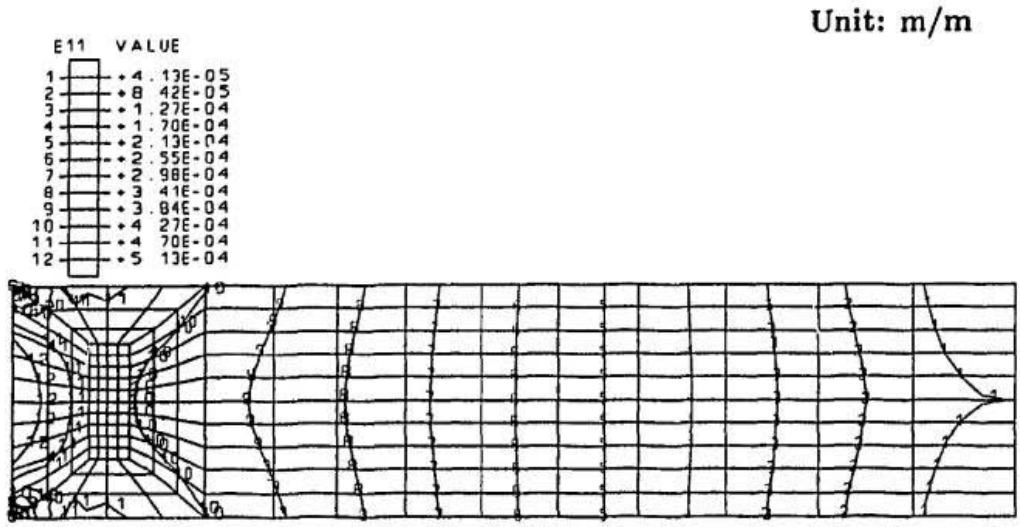

Figure 3.8: Contours of the surface strain ϵ_x without a surface Crack

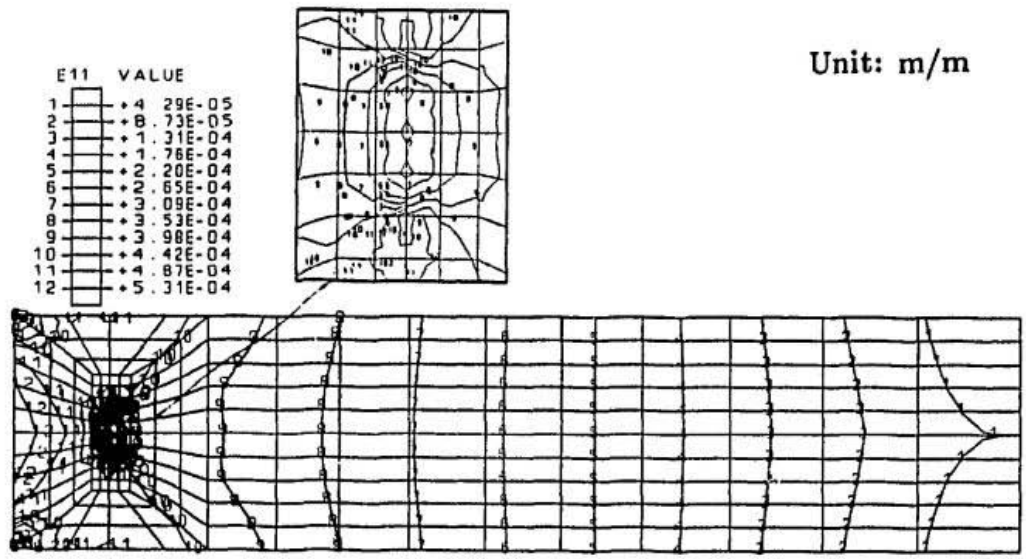

Figure 3.9: Contours of the surface strain ϵ_x with a surface crack

Table 3.1: Strain values ϵ_x for the uncracked and cracked plate around the crack

x coord(mm)	dis to the crack(mm)	$\epsilon_x(\mu\epsilon)$(uncracked)	$\epsilon_x(\mu\epsilon)$(cracked)	changes(%)
15.4	47.1	5.44	5.20	4.41
32.8	29.7	4.94	4.79	3.04
46.7	15.8	4.66	4.25	8.80
54.7	7.80	4.46	3.53	20.9
60.9	1.60	4.41	2.76	37.4
67.2	4.70	4.35	3.07	29.4
73.4	10.9	4.31	3.71	13.9
84.8	22.3	4.22	4.17	1.18
100.	37.5	4.13	4.18	-1.21
120.	57.5	4.02	4.08	-1.49
156.	93.5	3.80	3.83	-0.79

note: the origin of x-axis is at the fixed end; x coordinate for the crack $x_c = 62.5mm$.

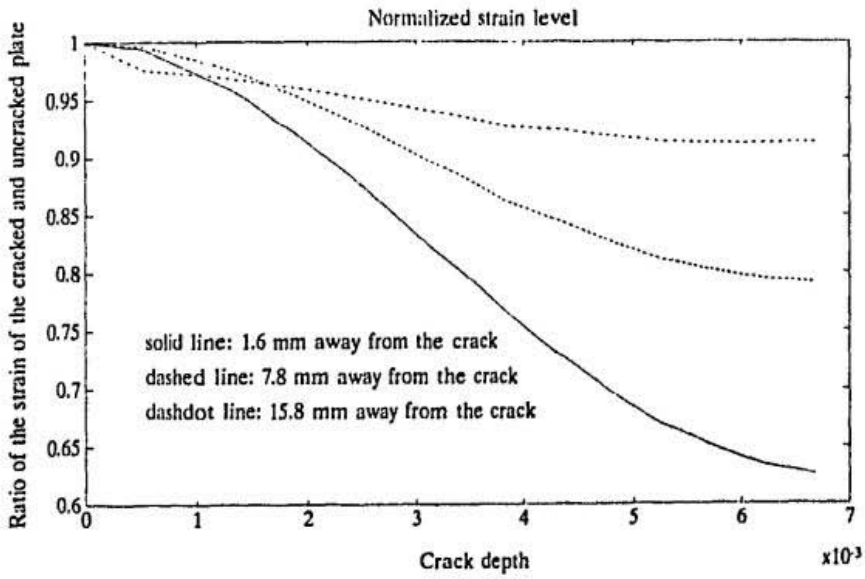

Figure 3.10: The normalized strain level decrease as the depth of the surface crack increases

are dependent on the amplitude of applied forces. In order to get a good and reliable results from experimental measurements, the applied forces must be large enough; also the applied forces must be the same for the uncracked and cracked structure.

3.2.2 Out-of-plane and Surface Displacements

The largest displacement component of the plate with the vertical load at the end is the out-of-plane displacement w; hence displacement w is studied first. Figs. 3.11 and 3.12 show the displacement contours of w of the uncracked and cracked plates. It is observed that there is very little difference between these two sets of contours; this indicates that the out-of-plane displacement is not sensitive to the presence of a small surface crack.

Corresponding to the surface strains considered early, the in-plane surface displacements u, at the surface of the plate, are determined. The in-plane surface displacements u, with and without the surface crack, are calculated and output. As mentioned before, ABAQUS cannot compute the surface displacements of shell element directly. So Eqn. (3.8) or (3.9) is used. In this particular case, the displacement at reference surface (which is the neutral axis) is almost zero; consequently Eqn. (3.9) is used. Since the thickness

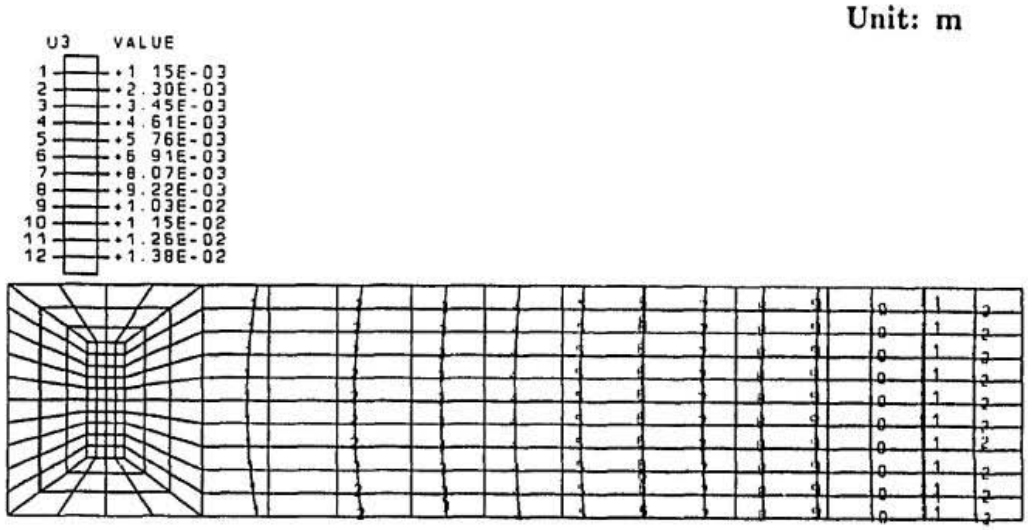

Figure 3.11: Contours of displacement w of the uncracked plate

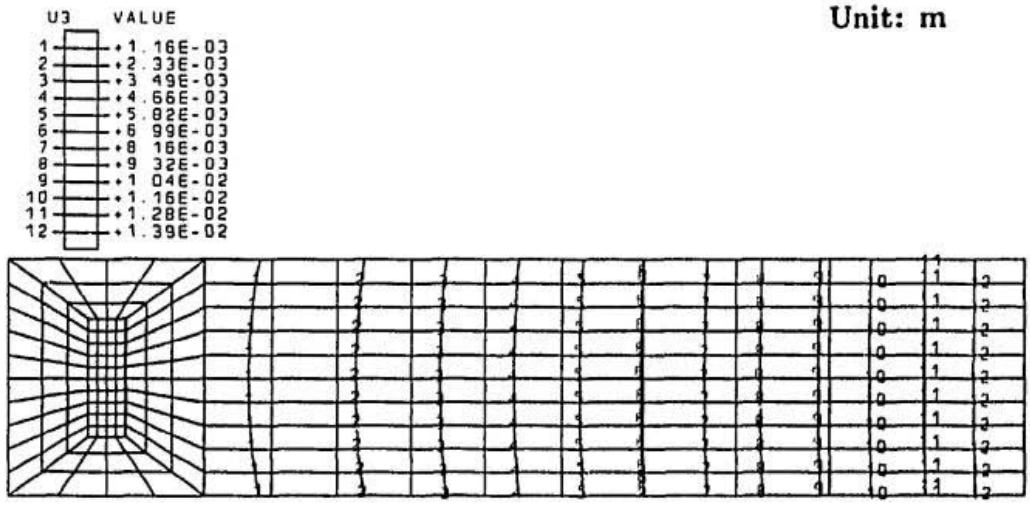

Figure 3.12: Contours of displacement w of the cracked plate

of the plate is a constant, the surface displacements are proportional to the corresponding rotations at the reference surface; hence the contours of rotation, at the reference surface, tend to show the same pattern as the corresponding surface displacement.

Figs. 3.13 and 3.14 give the contours of the rotation about the y-axis at the reference surface without/with the surface crack (which are proportional to the surface displacement u and show the same pattern). The crack depth is taken to be 70% of the thickness of the plate. It is observed that there are some increases in the x-axis surface displacements (given by the rotational degree of freedom of the element) at the center of the crack. In comparison to the surface strains (shown in Figs. 3.8 and 3.9), the change in the surface displacement field is small. Therefore for practical measurements, strain measurements give a better method for crack detection.

Fig. 3.15 shows the contours of the in-plane displacement u at the reference surface due to the presence of a crack. It is observed that there are many displacement contours around the crack; this is due to the change of in-plane displacements, after the surface crack was introduced. It should be pointed out that these values are very small compared to the corresponding rotations at the reference surface and the in-plane surface displacements. Moreover, even though the middle plane displacements u show quite a few interesting details

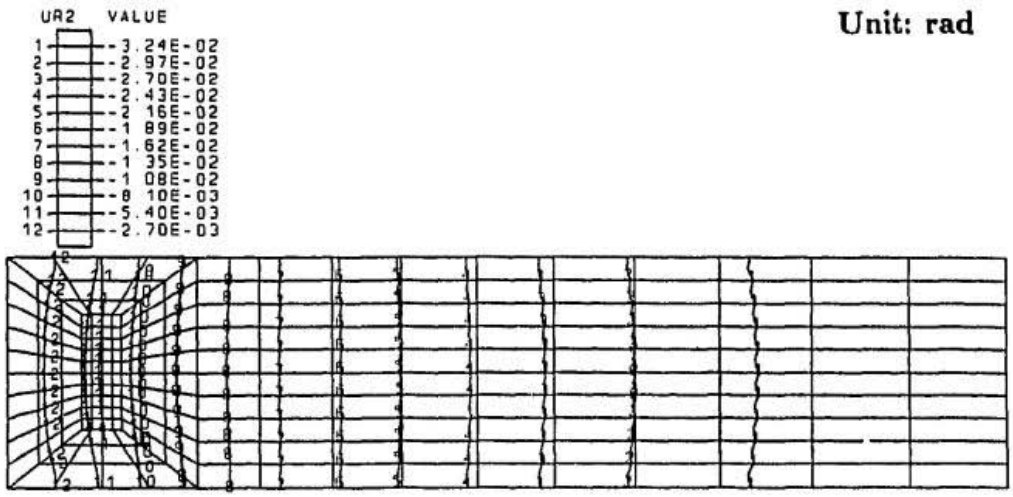

Figure 3.13: Contours of the rotation ϕ_y without the crack

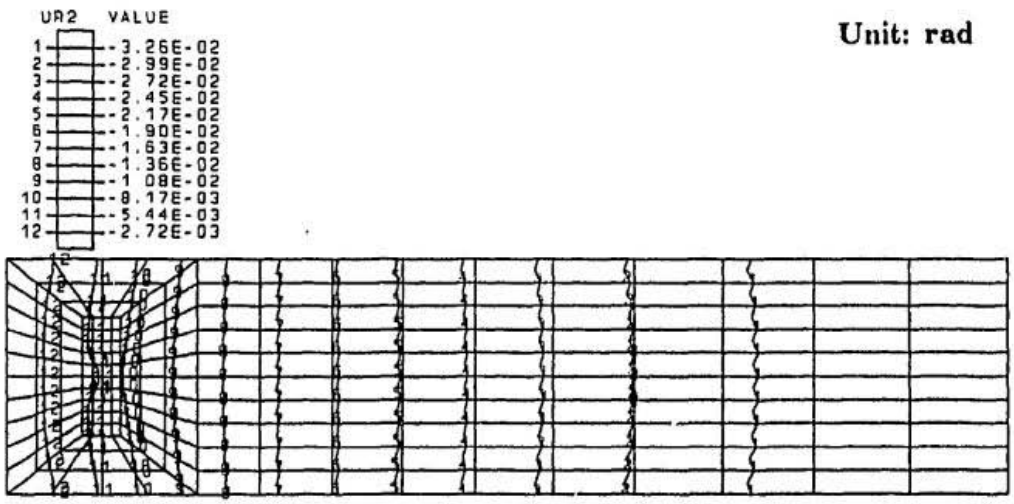

Figure 3.14: Contours of the rotation ϕ_y with the crack

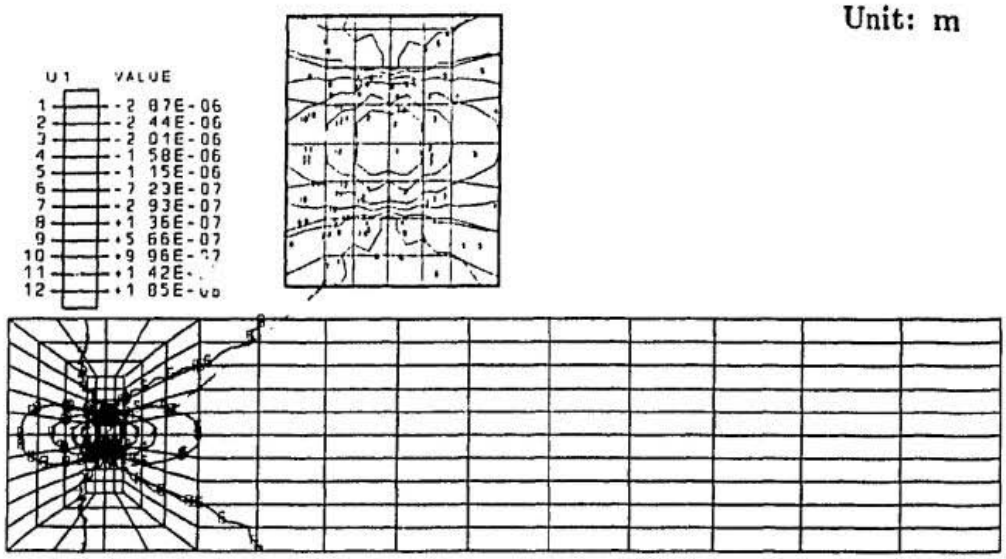

Figure 3.15: Contours of displacement u at the reference surface for a cracked plate

in displacement variation, this cannot be sensed by any sensing device; also these values are very small.

3.3 Summary

Cracks occurring in a structure change the stress/strain and displacement fields around the cracks. Among these changes a large decrease of surface strain, within a certain area around the crack, has been observed in this study. Therefore it is possible to apply strain gauges to real structures to detect cracks occurring in the structure. Further investigation involving dynamic

measurements and modal analysis are carried out in the following chapters to find out the best method for crack detection in real structures.

Chapter 4

Steady State Analysis of a Plate with a Surface Crack

4.1 Modal analysis and Frequency Response Function

4.1.1 Theoretical Basis

The modal analysis deals with the method of determining the basic vibration properties of a general linear structure. It is based on the concept that the structure's behaviour can be described by a set of vibration modes: the modal

model. This model is defined by a set of natural frequencies with corresponding vibration mode shapes and modal damping factors.

For the typical theoretical route to vibration analysis (by modal analysis), one begins with the description of the structure's physical characteristics, usually in terms of its mass, stiffness and damping properties. Then an analytical modal analysis is performed, and the modal model is determined. Finally, the response of the structure to a given excitation is obtained.

The governing equations of vibration for the structure are expressed as:

$$[M]\{\ddot{X}\} + [C]\{\dot{X}\} + [K]\{X\} = \{F(t)\} \tag{4.1}$$

where [M], [C] and [K] are the mass, damping and stiffness matrices, respectively, $\{X\}$ is the displacement vector and F(t) is the applied time-dependent force.

Applying Laplace transform to the equations:

$$\mathrm{L}([M]\{\ddot{X}\} + [C]\{\dot{X}\} + [K]\{X\}) = \mathrm{L}(\{F(t)\}) \tag{4.2}$$

one obtains:

$$([M]s^2 + [C]s + K)\{X(s)\} = \{F(s)\} + ([M]s + [C])\{X(0)\} + [M]\{\dot{X}(0)\} \tag{4.3}$$

or

$$[B(s)]\{X(s)\} = \{F(s)\} + ([M]s + [C])\{X(0)\} + [M]\{\dot{X}(0)\} \tag{4.4}$$

Rearrangement of the above equation leads to

$$\{X(s)\} = [H(s)](\{F(s)\} + ([M]s + [C])\{X(0)\} + [M]\{\dot{X}(0)\}) \tag{4.5}$$

where [H(s)] = $[B^{-1}(s)]$ is called the transfer function matrix.

For the homogeneous solution:

$$[B(s)]\{X(s)\} = 0 \tag{4.6}$$

The characteristic polynomial equation is obtained from:

$$p(s) = det[B(s)] = 0 \tag{4.7}$$

Here the Laplace variable $s = \sigma + j\omega$

The roots of the characteristic equation (s_i) are called eigenvalues. Substituting an eigenvalue into the equation of motion and solving for U yields the associated eigenvector:

$$[B(s_i)]\{U_i\} = \{0\} \tag{4.8}$$

where s_i is the eigenvalue and U_i is the associated eigenvector. The eigenvalue s_i (or sometimes called complex natural frequency) has two parts: (i) the imaginary part which gives the damped natural frequency; (ii) the real part which gives the damping factor.

It can be shown that modal vectors are orthogonal with respect to one another if they are weighted with respect to the stiffness matrix [K] and mass

matrix [M]. It can also be shown that modal vectors are orthogonal to one another if they are weighted with respect to the damping matrix [C], when the damping matrix is proportional to the mass matrix and stiffness matrix (the proportionally damped system).

Eqn. (4.1) can be written in the modal space. The transformation from physical space to modal space is given by

$$\{X\}_{n\times 1} = [U]_{n\times m}\{p\} \tag{4.9}$$

where:

$\{X\}$: displacement of the physical degrees of freedom.

$[U]$: modal matrix. $[U] = [U_1, U_2, ...U_m]$.

$\{p\}$: displacement in modal space.

n: number of physical degrees of freedom.

m: number of modes evaluated.

Using Eqn. (4.9), Eqn. (4.1) can be written as:

$$[M][U]\{\ddot{p}\} + [C][U]\{\dot{p}\} + [K][U]\{p\} = \{F(t)\} \tag{4.10}$$

Pre-multiplying by $[U]^T$, we get:

$$[U]^T[M][U]\{\ddot{p}\} + [U]^T[C][U]\{\dot{p}\} + [U]^T[K][U]\{p\} = [U]^T\{F(t)\} \tag{4.11}$$

For the proportionally damped system, using the orthogonality properties of the modal vectors weighted with respect to the mass, stiffness and damping matrices, one can define the diagonal modal mass matrix as:

$$[\overline{M}]_{modal} = [U]^T[M][U]$$

diagonal modal damping matrix as:

$$[\overline{C}]_{modal} = [U]^T[C][U]$$

diagonal modal stiffness matrix as:

$$[\overline{K}]_{modal} = [U]^T[K][U]$$

and modal force vector as:

$$\{\overline{F}\}_{modal} = [U]^T\{F\}$$

Rewriting Eqn. (4.1) as:

$$[\overline{M}]_{m\times m}\{\ddot{p}\}_{m\times 1} + [\overline{C}]_{m\times m}\{\dot{p}\}_m + [\overline{K}]_{m\times m}\{p\}_{m\times 1} = \{\overline{F}\}_m \qquad (4.12)$$

one can notice that each equation is uncoupled from the other equation and represents an individual modal response of the system (Ewins, 1984).

4.1.2 Frequency Response Function

From Eqn. (4.5), if one assumes a zero initial condition, one obtains:

$$[H(s)] = \frac{\{X(s)\}}{\{F(s)\}} \qquad (4.13)$$

Let the Fourier variable $s = j\omega$, then we have:

$$[H(j\omega)] = \frac{\{U(j\omega)\}}{\{F(j\omega)\}} \tag{4.14}$$

where $[H(j\omega)]$ is called the Frequency Response Function (FRF)

The frequency response function has many forms in terms of input (excitation) and output (response). The traditional forms include:

(a) receptance, in the form of (displacement)/(force), where displacement is the output.

(b) mobility, in the form of (velocity)/(force), where velocity is the output.

(c) inertance, in the form of (acceleration)/(force), where the acceleration is the output.

In all cases, the input is the excitation force.

Recently, the consideration of surface strains has been introduced into modal analysis. The strain frequency response function means the transform function between input (the excitation force) and output (the strain level at a certain point) in frequency domain. The strictly theoretical definition can be found in the articles of Bernasconi and Ewins (1989), and Li (1989). In this study, the strain FRFs are analyzed in the same manner as the displacement or acceleration FRFs. An unit force is applied to the plate, then steady state

linear dynamic analysis is performed by assigning a specific range of frequencies. The exciting force will be varying within the range of the frequencies considered in the study. The strain response, as well as the displacement and acceleration responses will be determined in the frequency domain. Thus the frequency response functions of strain, displacement, and acceleration are obtained. The modal strains are defined as the strains measured at the different response points of the structure, when the structure is excited by a unit force at a resonant frequency.

4.2 Change of Modal Parameters Due to the Growth in Depth of the Surface Crack

4.2.1 Global Changes of the Modal Parameters

It is known that any crack or damage occurring in the structure will affect the physical properties of the structure. The changes in physical properties will be shown by the changes in modal parameters. These modal parameters are independent of the amplitude of applied forces. Earlier studies on cracking of structures had focused only on the natural frequency changes. But these changes of natural frequencies are very small, although not impossible to mon-

Table 4.1: Frequency changes due to the growth of the depth of the surface crack

Crack depth D(mm)	ω_1(Hz)	ω_2(Hz)	ω_3(Hz)	ω_4(Hz)	ω_5(Hz)	ω_6(Hz)	ω_7(Hz)
0	18.991	118.62	125.57	332.65	367.75	391.99	653.02
0.00048	18.989	118.62	125.57	332.64	367.75	391.97	653.01
0.00095	18.985	118.61	125.56	332.63	367.75	391.96	653.01
0.00140	18.979	118.59	125.56	332.62	367.74	391.95	653.01
0.00191	18.971	118.57	125.55	332.61	367.74	391.93	653.01
0.00238	18.961	118.55	125.54	332.59	367.73	391.91	653.01
0.00286	18.951	118.52	125.54	332.58	367.73	391.89	653.01
0.00333	18.939	118.49	125.53	332.56	367.72	391.88	653.01
0.00381	18.923	118.45	125.53	332.53	367.71	391.86	653.00
0.00429	18.915	118.43	125.53	332.52	367.70	391.85	653.00
0.00476	18.903	118.40	125.52	332.50	367.69	391.84	653.00
0.00523	18.890	118.37	125.52	332.48	367.68	391.83	653.00
0.00571	18.880	118.35	125.52	332.46	367.67	391.83	653.00
0.00619	18.870	118.32	125.51	332.44	367.65	391.82	653.00
0.00667	18.862	118.30	125.51	332.43	367.43	391.82	653.00

itor. A certain amount of frequency shift would occur only when a large crack has formed in the structure.

In this study, natural frequencies of the plate are determined through the eigenvalue extraction procedure given by ABAQUS. The natural frequency shifts due to the growth of the depth of the surface crack (each crack depth increase constitutes a 5% change in crack depth) are calculated and shown in Table 4.1. It is observed that even for the largest crack depth change, which occurs for the first mode, the frequency changes by less than 1%. The corresponding surface crack is 6.667 mm deep, 40 mm long; the plate is 650

mm long, 200 mm wide, and 9.525 mm thick.

The mode shapes corresponding to these natural frequencies are shown in Fig. 4.1 (uncracked plate). It is observed that the first, second, fourth and seventh modes are bending modes; and the third and sixth modes are torsion modes; the fifth mode is the transverse mode.

The analytical modal analysis is also carried out to determine the global changes of modal parameters due to increase in crack depth. The frequency range is chosen to vary from 1 to 700 Hz, which includes the first seven resonant frequencies. The accelerations and displacements obtained at the free end, far away from the surface crack, are chosen to represent the global parameters. The acceleration FRFs and displacement FRFs at the centre of the free end are calculated and plotted. In the modal analysis, a unit vertical excitation force is applied to the corner of the free end of the plate. The response measurements for the acceleration and displacement are obtained at the centre of the free end. Therefore, in the frequency response functions, the bending modes will be dominant while the response corresponding to the torsion modes will be small, and the response corresponding to the transverse mode will be almost zero. Figs. 4.2 and 4.3 show the acceleration and displacement FRFs of uncracked plate and the plate with the largest crack depth. In the calculation of the FRFs, a damping ratio of 1% was introduced into the system.

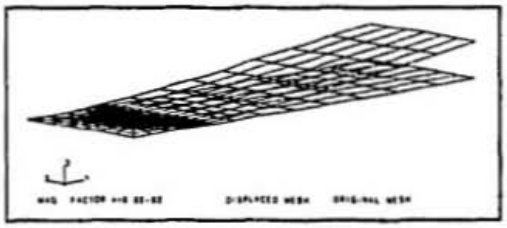

ω_1

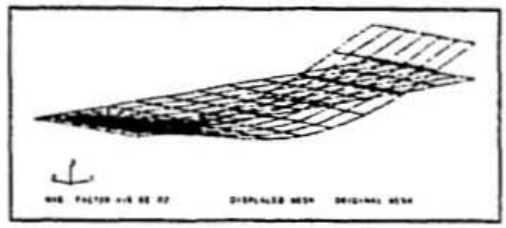

ω_2

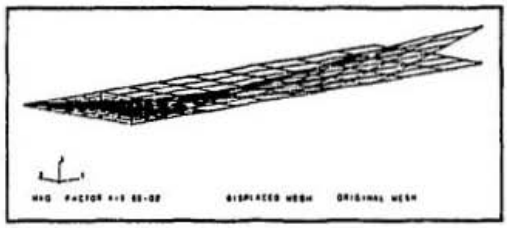

ω_3

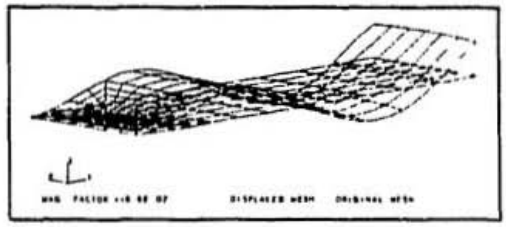

ω_4

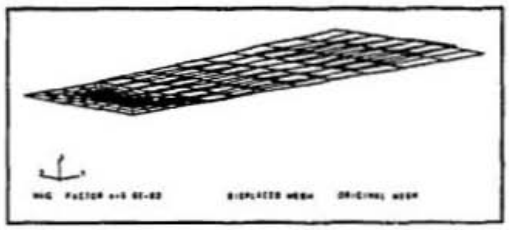

ω_5

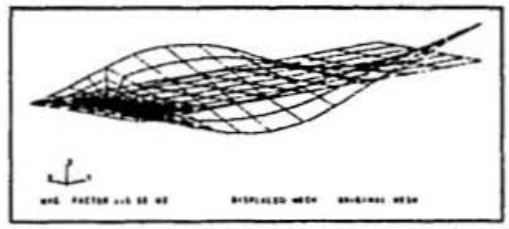

ω_6

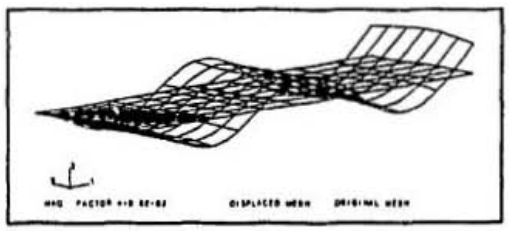

ω_7

Figure 4.1: Mode shapes of the uncracked plate

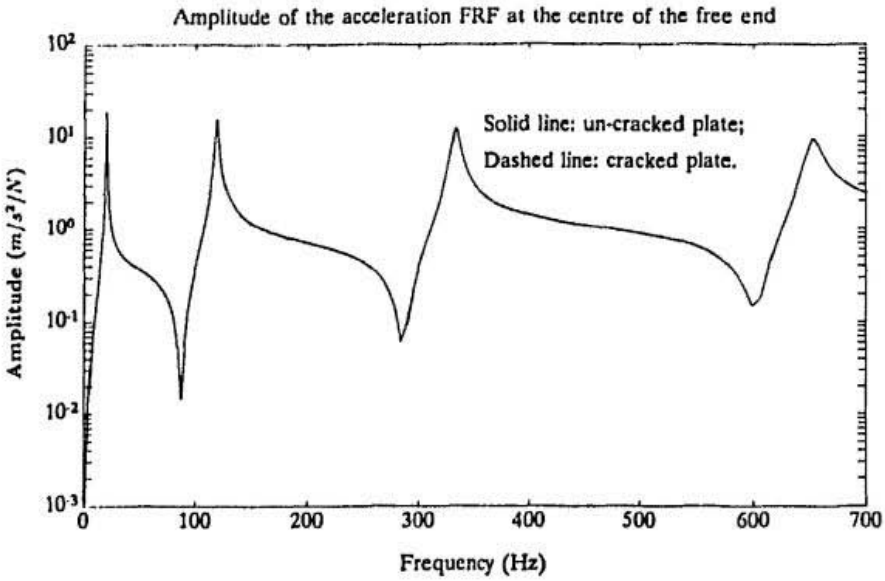

Figure 4.2: Acceleration FRFs of uncracked and cracked plates

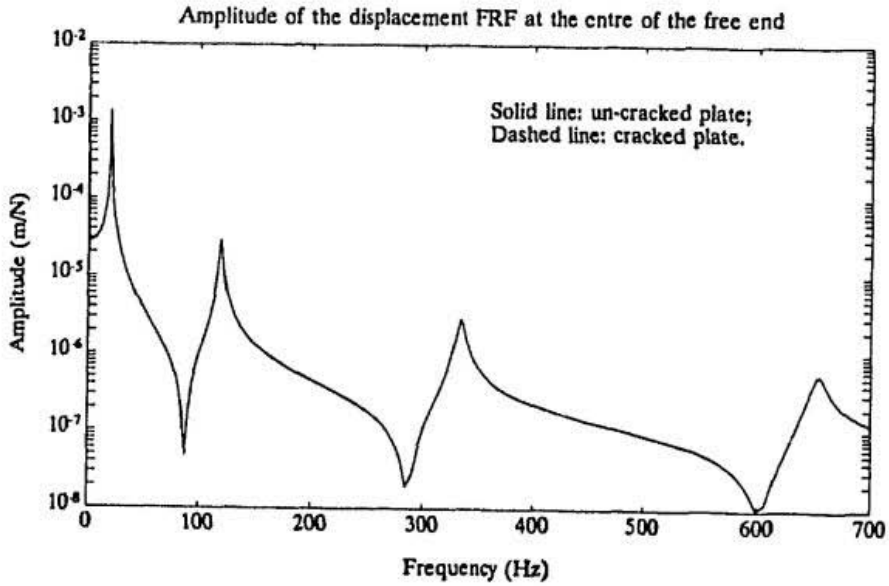

Figure 4.3: Displacement FRFs of uncracked and cracked plates

Table 4.2: Changes of the amplitude of displacement and acceleration FRFs at resonant frequencies at the centre of the free end

	1st mode	2nd mode	3rd mode	4th mode
Acc. Ampl.($m/s^2/N$) (uncracked)	19.229	15.617	12.459	9.4495
Acc. Ampl.($m/s^2/N$) (cracked)	19.187	15.638	12.479	9.448
Change (%)	0.22	-0.11	-0.16	0.02
Dis. Ampl.(mm/N) (uncracked)	1.3506	0.0281	0.0029	0.0006
Dis. Ampl.(mm/N) (cracked)	1.3660	0.0283	0.0029	0.0006
Change (%)	-1.11	-0.71	0.00	0.00

As could be seen from Figs. 4.2 and 4.3, it is observed that there is almost no difference between the two curves for cases of with and without the crack. Table 4.2 gives changes of the amplitude of displacement and acceleration FRFs at each resonant frequency. The largest amplitude change occurs at the first resonant frequency of the displacement FRF, and the change is less than 1.2%. Also as seen from Table 4.1, the largest frequency shift is less than 1%. However from an earlier study on a more complex structure (Chen and Swamidas, 1992) with a larger crack, it was observed that it was possible to monitor the global changes from global sensors such as accelerometers or linear variable displacement transducers. In that experiment, a 2% of natural frequency shift was observed. From that experimental investigation and other similar studies considered earlier (Chondros et al. 1980 and 1989, Collins et al. 1991 and 1992, Ilanko et al. 1991, Gomes et al. 1990 and 1991, and

Guigne et al. 1992), one can conclude that it is possible to sense the cracking in any structure by observing the changes in natural frequencies that occur in the global sensors. In the present study since the cracking is very small, a shielding of its presence occurs in the overall vibration response; the structure vibrates in a global manner as if no crack is present in it. Hence the changes in the FRF are very marginal.

It has been stated by earlier researchers that damping ratios of the structure, at different resonant frequencies, change considerably due to cracking. Sanliturk et al. (1991) reported a theoretical study of the damping produced by fatigue cracks. The damping increase due to a fatigue crack in beam-like structures was predicted. A rubbing damping model of energy dissipation was considered in their study. However, from the earlier experiment conducted in the Strength Laboratory at Memorial University (Chen and Swamidas, 1992), the change of damping ratios did not always increase, but sometimes it also decreased. It was concluded from that experiment that damping changes due to crack growth needed more studies owing to the complex mechanism of damping in real structures. It was also shown that the other modal parameters such as amplitudes and mode shape undergo changes due to cracking in structures. Based on the fact mentioned above, a constant damping ratio of 1% was chosen for all resonant frequencies in this study.

Once the frequency shifts are observed from the global sensors, the next step will be to determine where the crack is located and how severe it is. But for the determination of the location and severity of the crack that occurs in the structure, monitoring of the global changes in the modal parameters such as natural frequencies alone is not enough. Because the same amount of frequency shift may be caused by cracks at different locations having different depths or lengths, one needs to have a procedure to determine the location and severity of cracking. Hearn et al. (1991) proposed a method by comparing the ratio of changes in natural frequencies to the member characteristic ratio ensembles. However, this method is limited to skeletal structures such as welded frames or bridges, and only the damaged member of the skeletal structure can be identified. From the literatures reviewed and the experimental study carried out earlier at Memorial University, it appears that the most sensitive set of modal parameters will be the set of local modal parameters; and one of these local parameters will be the strain level around the crack and the nearby area.

4.2.2 Local Changes of the Modal Parameters

The crack in the structure will change the dynamic properties of the structure. This effect will be more significant in the local area around the crack than in any other area of the structure. Since modal parameters, whether at the local or global level, represent the structural properties, monitoring of the local changes of the modal parameters will give a more direct and significant indication of the crack occurring in the structure. In the classical modal theory, modal parameters normally mean natural frequencies, damping factors and displacement mode shapes. Normally, these parameters have only a global meaning. For example, the natural frequencies usually mean the resonant frequencies for the whole structure.

Since strain modal testing has been used in this study, the local strain values can also be designated as an important local parameter. When one observes the strain FRFs, the locations of the peaks indicate the resonant frequencies of the structure. These resonant frequencies will be the same throughout the structure. The local effects will affect only the amplitudes of the peaks of the strain FRF functions. The amplitude of the strain FRFs measured from a local area close to the crack is different from the FRFs from any other area in the structure. This local strain FRFs contain information of the particular

crack and can be utilized to indicate the location and severity of the crack. Therefore by performing strain modal analysis or testing, recording the strain FRFs in the local area at different times, or at different crack depths in an analytical investigation and comparing the new FRFs with previous ones, it is possible to find out the location and severity of the crack in the structure.

Based on the method discussed above the strain response functions of the plate, with and without crack, are calculated. Steady state analysis is performed with a harmonic excitation whose frequencies range from 1 to 700 Hz. The response is calculated in the frequency domain, with a unit force input, and thus the strain frequency response functions are obtained.

Three measurement points for strain response outputs are chosen. The distance from the measurement points to the crack are 1.6 mm, 7.8 mm and 15.8 mm, respectively. Figs. 4.4, 4.5 and 4.6 show the strain FRFs for the uncracked plate and for the plate with the largest crack depth (70% of the thickness of the plate). Figs. 4.4, 4.5, and 4.6 are the FRFs determined at distances of 1.6 mm, 7.8 mm and 15.8 mm away from the crack, respectively. Significant changes of the amplitude of the strain FRFs are observed. This indicates that the local effect has a strong influence on the amplitude of the strain FRFs. Table 4.3 gives the changes of the amplitude of strain FRFs at each resonant frequency. It is observed that for the point 7.8 mm away from

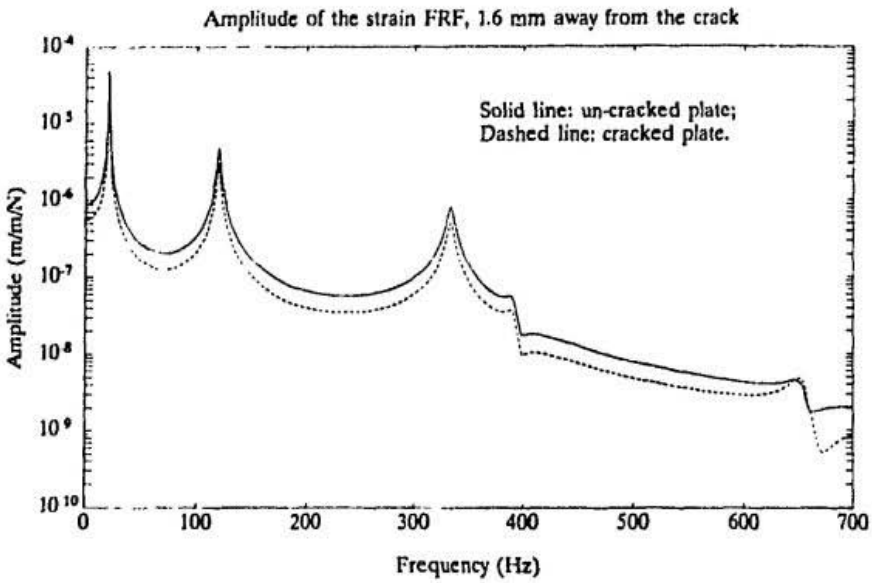

Figure 4.4: Strain FRFs, 1.6 mm away from the crack

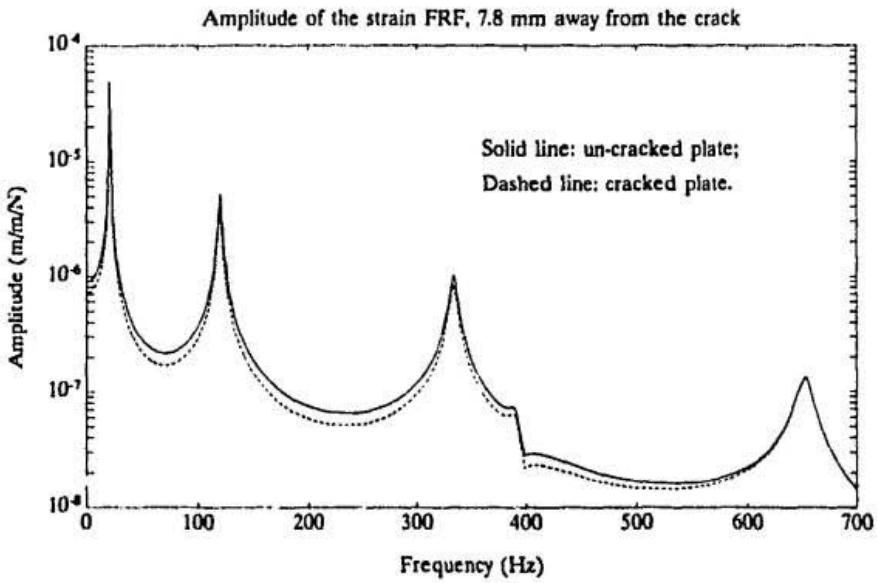

Figure 4.5: Strain FRFs, 7.8 mm away from the crack

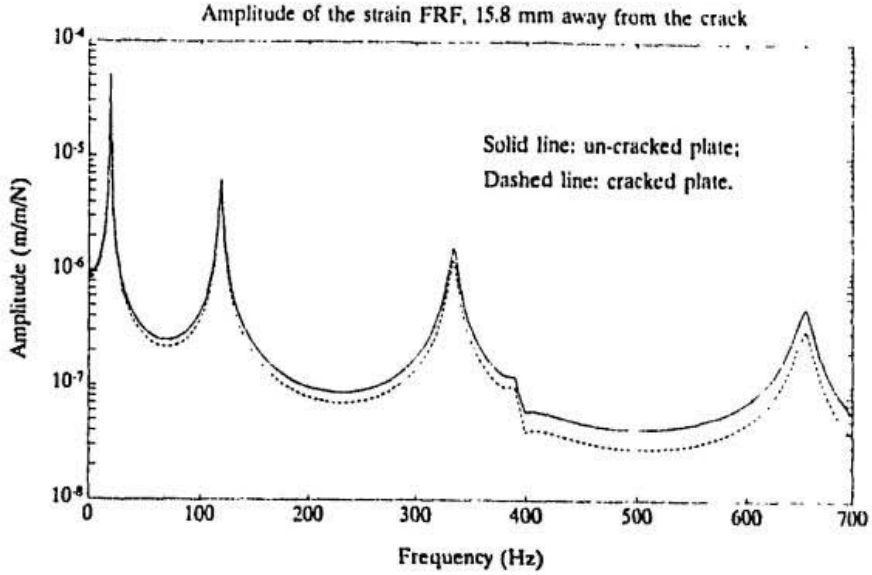

Figure 4.6: Strain FRFs, 15.8 mm away from the crack

the surface crack, the changes of the amplitudes of the strain FRFs are 21.0%, 20.9% and 18.6% for the first, second and third bending modes, respectively. From the earlier static analysis, the same crack depth at the same measurement point caused a static strain decrease of 20.9%. Hence from the results of the first three modal responses, there dose not seem to be any appreciable difference between the results of static and dynamic strain gauge testing. Results from the measurement point 15.8 mm away from the crack, show changes of 9.25%, 14.8%, 22.1% and 36.3% for the first four bending modes, from the results of modal analysis given in Table 4.3. The static measurements given earlier show a 8.8% change at this point. Therefore, strain modal testing gives

Table 4.3. Changes of the amplitude of strain FRFs

Dis. from the crack	1.6 mm			7.8 mm			15.8 mm		
Bending mode	uncr.	cr.	%	uncr.	cr.	%	uncr.	cr.	%
1st ($\mu\epsilon/N$)	48.14	30.06	37.6	49.00	38.73	21.0	51.69	46.91	9.25
2nd ($\mu\epsilon/N$)	4.819	2.955	38.7	5.223	4.129	21.0	6.287	5.356	14.8
3rd ($\mu\epsilon/N$)	0.816	0.498	39.0	1.031	0.839	18.6	1.592	1.240	22.1
4th ($\mu\epsilon/N$)	0.004	0.004	0.0	0.130	0.128	1.54	0.471	0.300	36.3

a better indication of the crack occurring in the structure at this measurement point.

It must also be observed from Figs. 4.4-4.6, that the changes in the strain levels of the FRF in the nonresonant regions due to cracking are appreciable as shown in Table 4.4. The changes at nonresonant points indicates changes similar to the static values at the two points nearest to the crack, viz., at 1.6 mm and 7.8 mm away from the crack; but at 15.8 mm away from the crack, the changes are once again much higher than the static ones. Probably an acoustic mode of crack detection during modal testing may be able to sense these changes due to cracking better in the nonresonant regions.

Fig. 4.7 gives the waterfall plot of the strain FRF changes against the increase in the depth of the crack for the first three bending modes. The modal strain value is normalized against the corresponding peak modal strain FRF of uncracked plate. The measurement point is 7.8 mm away from the crack. It is

Table 4.4: Changes in amplitudes of strain FRFs at nonresonant points

Dis. away from the crack	Freq. (Hz)	69.86	231.6	525.8
1.6 mm	uncracked	2.0437e-7	5.7271e-8	6.457e-9
	cracked	1.2578e-7	3.4682e-8	4.0183e-9
	change(%)	38.45	39.44	37.77
7.8 mm	uncracked	2.1621e-7	6.5248e-8	1.6219e-8
	cracked	1.7004e-7	5.1455e-8	1.4472e-8
	change(%)	21.35	21.14	10.77
15.8 mm	uncracked	2.4819e-7	8.5760e-8	4.2173e-08
	cracked	2.1502e-7	6.9926e-8	2.8400e-8
	change(%)	13.36	18.46	32.66

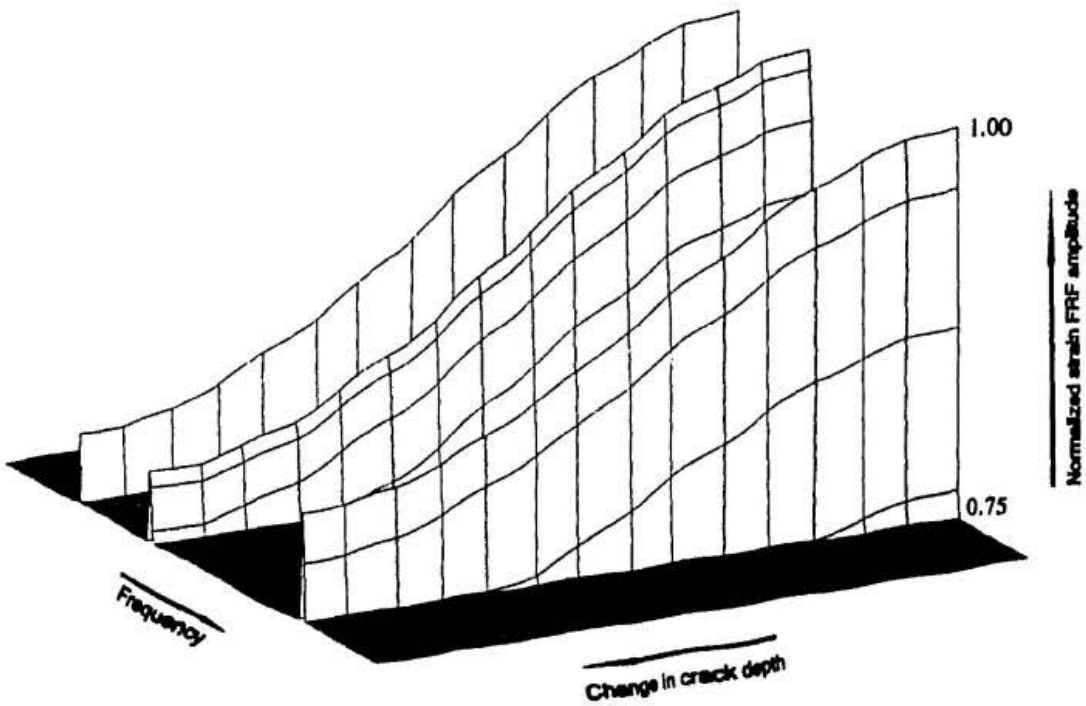

Figure 4.7: Waterfall plot of strain FRFs, 7.8 mm away from the crack

observed that a clear trend of decrease of the amplitude of the strain FRFs occurs as the surface crack depth grows.

When carrying out an analytical investigation, one knows where the crack is located; consequently one can state confidently where the local area is. But in a real structure, the location of the crack is unknown and one needs to determine where it is located from transducer measurements. Fortunately, for most of the structures, we can expect the cracks to occur around certain defined critical locations. These critical areas can be determined by an earlier finite element analysis carried out for the structural response. For example, in offshore platforms, the critical areas will be the highly stressed welded junctions of the structure. Thus we can define a certain amount of these areas as critical "local" areas. Monitoring of the strain FRFs in these critical "local" areas using strain gauges will give a clear indication of the location and severity of cracks that occur in the structure.

Chapter 5

Resonant and Transient Responses of The Plate With a Surface Crack

5.1 Sinusoidal Excitation

5.1.1 Time History

The procedure used to calculate the time history of the plate subjected to a sinusoidal or impulsive excitation is the modal superposition technique. As mentioned in the previous chapter the response of the structure can be ex-

pressed in terms of eigenmodes and the generalized modal displacements of the system. Only eigenmodes that are close to the frequencies of interest are required. In this study, the first seven modes are included in the modal superposition. For the linear dynamic response of the structure, the inclusion of seven modes are considered to give results which are accurate enough.

A sinusoidal excitation force with a constant frequency and amplitude is chosen for the excitation; when this frequency coincides with one of the natural frequencies of the structure, the excitation becomes a resonant one. The three natural frequencies corresponding to the first three bending modes are used as these resonant frequencies at which the structure is excited. Theoretically, when excited at the natural frequency, the structure will be resonant at this frequency, and will have the corresponding displacement mode shape; according to the definition of the modal strain given in the previous chapter, the normalized strain mode shape can also be obtained by calculating the corresponding strain values and normalizing them.

In order to obtain the bending modal strain shapes the excitation force is applied at the centre of the free end. The strain measurement points are located along the centre line of the plate. The strain response at the centre line of the plate 7.8 mm away from the crack, and the displacement response at the free end, are plotted in Figs.5.1-5.3 for the three resonant frequencies,

respectively. It can be observed from these response curves that there is an oscillating phenomenon associated with the responses at the second and third model responses. The excitation frequencies were chosen as the corresponding eigenvalues of the uncracked or cracked plate given in Table 4.1. In spite of the best effort made in the numerical signal analysis procedure, the oscillating behaviour persisted. Further discussions on this aspect are made in the next section.

Fig. 5.4 shows the strain response of the uncracked and cracked plate, when the plate is excited at the first resonant frequency (bending mode). The measurement point is 7.8 mm away from the crack. It is observed that the amplitude of the strain response decreases for the cracked plate from that of the uncracked one. This behaviour is as expected since from the static analysis, it is already known that there will be strain release in this area as the crack grows in depth. Since the response is directly related to the excitation force, any change in the excitation force will affect the response. Therefore the method which uses the strain response directly to detect cracking in the structure is less precise than the method using modal analysis, because modal parameters are independent to the amplitude of the excitation forces.

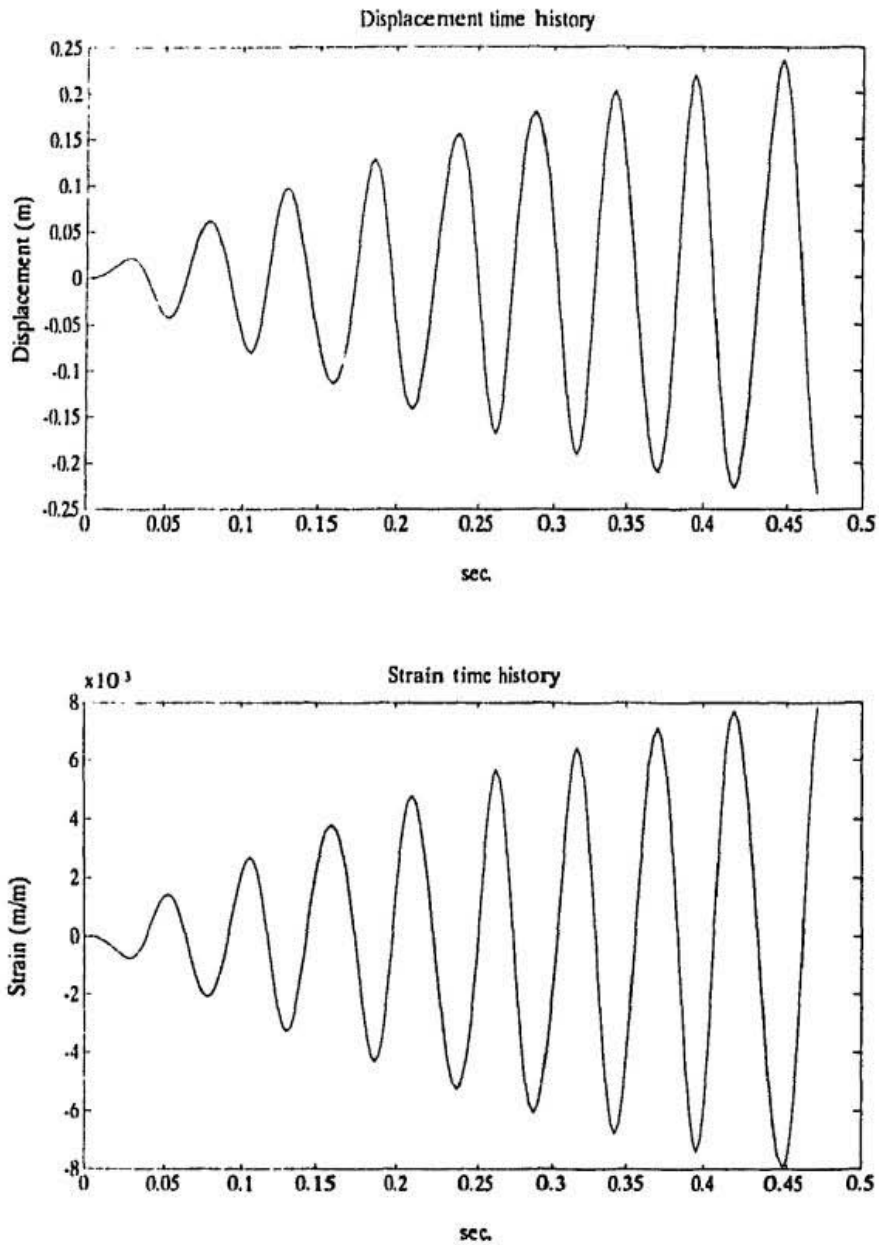

Figure 5.1: Displacement and strain responses for the first resonant excitation frequency

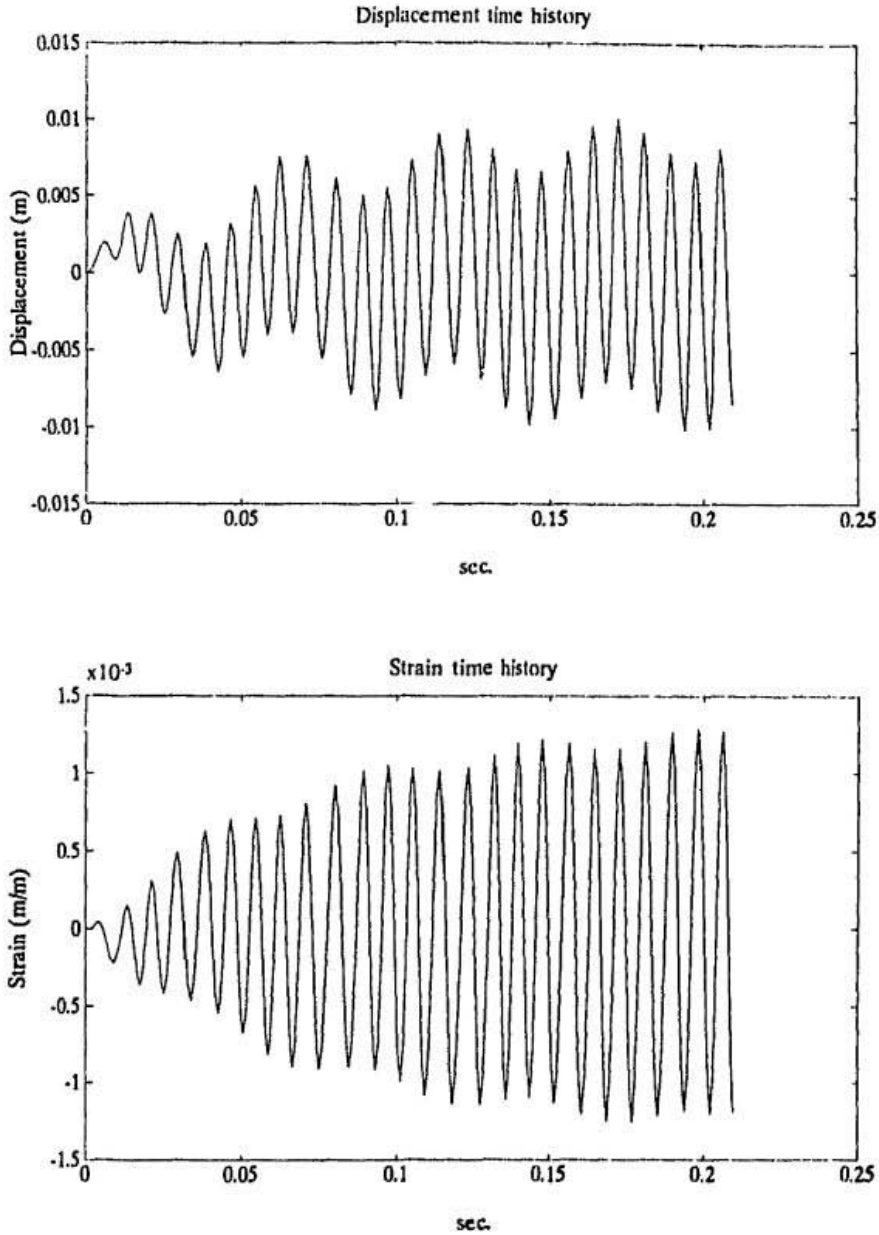

Figure 5.2: Displacement and strain responses for the second resonant excitation frequency

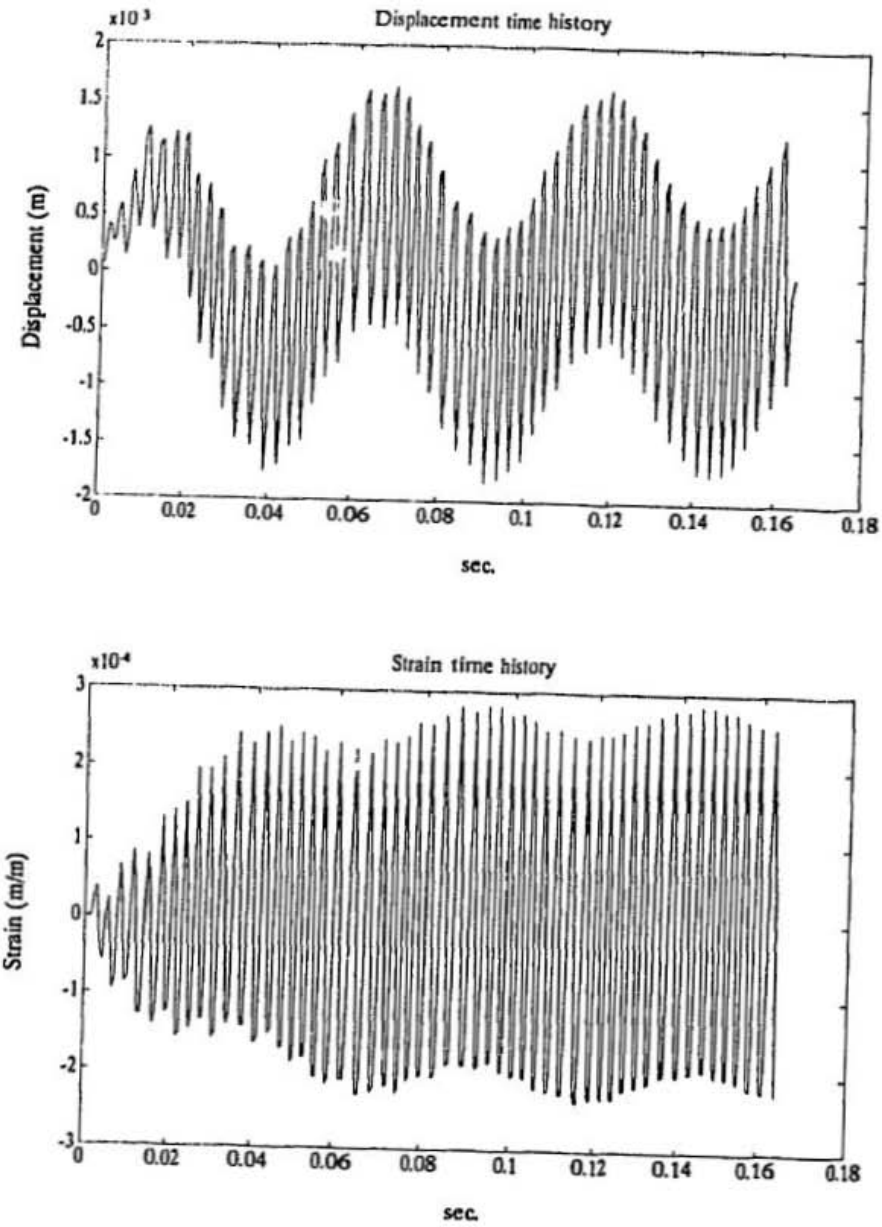

Figure 5.3: Displacement and strain responses for the third resonant excitation frequency

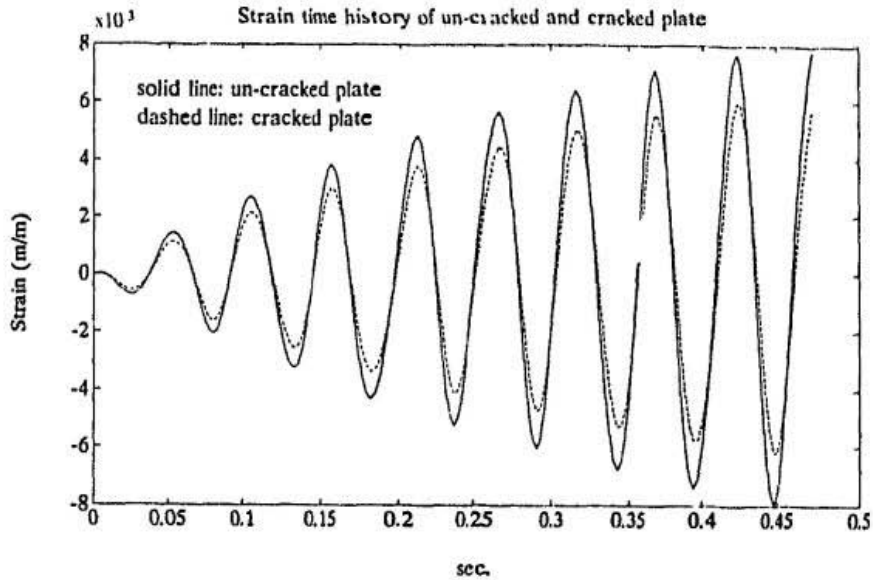

Figure 5.4: Strain responses of the uncracked and cracked plate, at a point 7.8 mm away from the crack, for the first bending modal frequency

5.1.2 Power Spectrum

From Figs.5.1-5.3, it is observed that besides the excitation frequency, the responses consist of other frequencies which cause an oscillating behaviour when the plate is excited at the second and third bending natural frequencies. This behaviour is clearly shown in the displacement responses of the figures cited above. Figs. 5.5-5.7 show the power spectrum of the responses given in Figs. 5.1-5.3, respectively. It is noticed that when the plate is excited at the first natural frequency, the responses occur only at that frequency; when the plate is excited at the second bending resonant frequency, the responses contain contributions from both the first and second natural frequencies, but the power for the second natural frequency is much higher than that for the first one; when the plate is excited at the third bending resonant frequency, the responses contain contributions from the first and second resonant frequencies besides the excitation frequency. Once again the power for the excitation frequency is higher than others. It is believed that these phenomena are caused by numerical errors in the computational procedures. The time increments for the time history calculations are 0.002633 sec, 0.0004215 sec, and 0.0003006 sec for excitation at the first, second and third bending resonant frequencies, respectively. In order to get the steady state response of the structure, the

time history must be calculated for a certain length of time. The time duration used in this study for the three excitations are 0.473909 sec, 0.2103285 sec, and 0.1635264 sec, respectively. When the excitation frequency is high, the time increment must be small to guarantee the results with a certain accuracy. Moreover the time required for the response to reach the steady state does not change much. This requirement causes difficulties for the computation of the time history for the high frequency excitation, when the available computer disk storage space and the CPU time are limited. Hence the time increments and time durations listed above, are based on the compromise of the accuracy due to the limitation on the computer disk storage space and the CPU time.

It should be pointed out that the frequency resolutions in the power spectra determination are coarse because of the limitation in the calculation of time histories. For the first mode, the resolution is 2.1218 Hz; while that for the second and third mode are 4.7450 Hz and 6.1152 Hz, respectively. That will explain why the peaks in the power spectra are not located exactly at the resonant frequencies. But to draw the power spectral distribution and to examine the trend of changes of the power spectrum as the crack depth develops, these resolutions are good enough.

From the power spectral responses, it is observed that for the strain responses, the power for the excitation frequency is much high than the others, even when

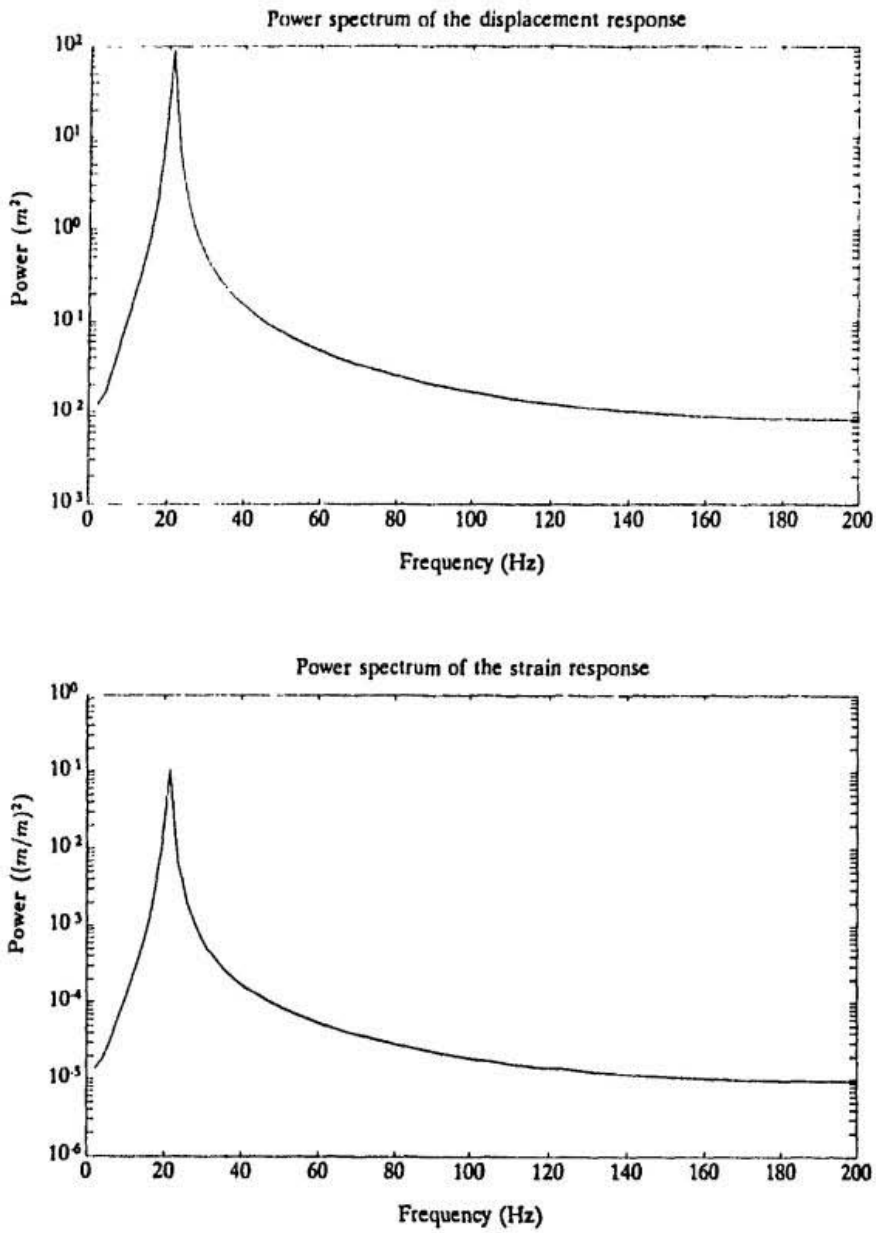

Figure 5.5: Power spectrum of the responses when excited at ω_1

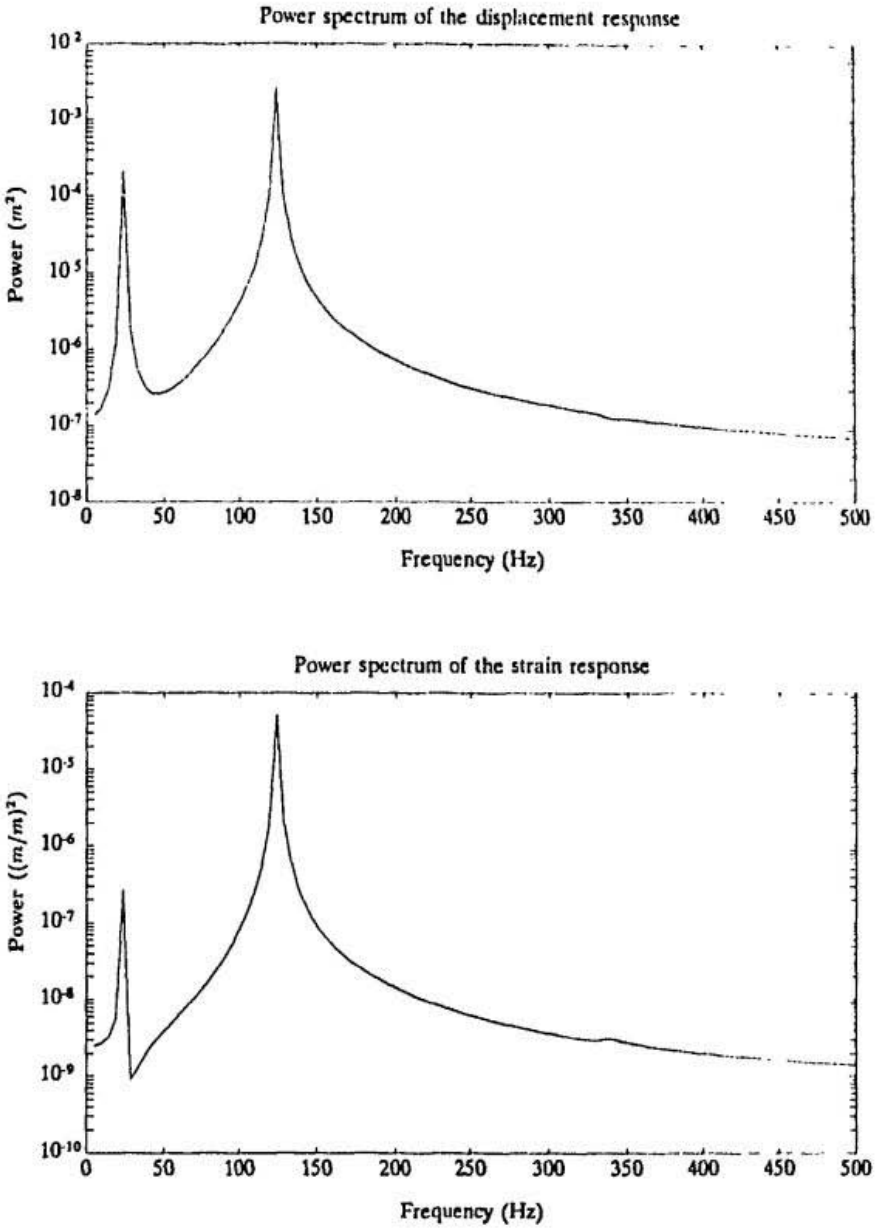

Figure 5.6: Power spectrum of the responses when excited at ω_2

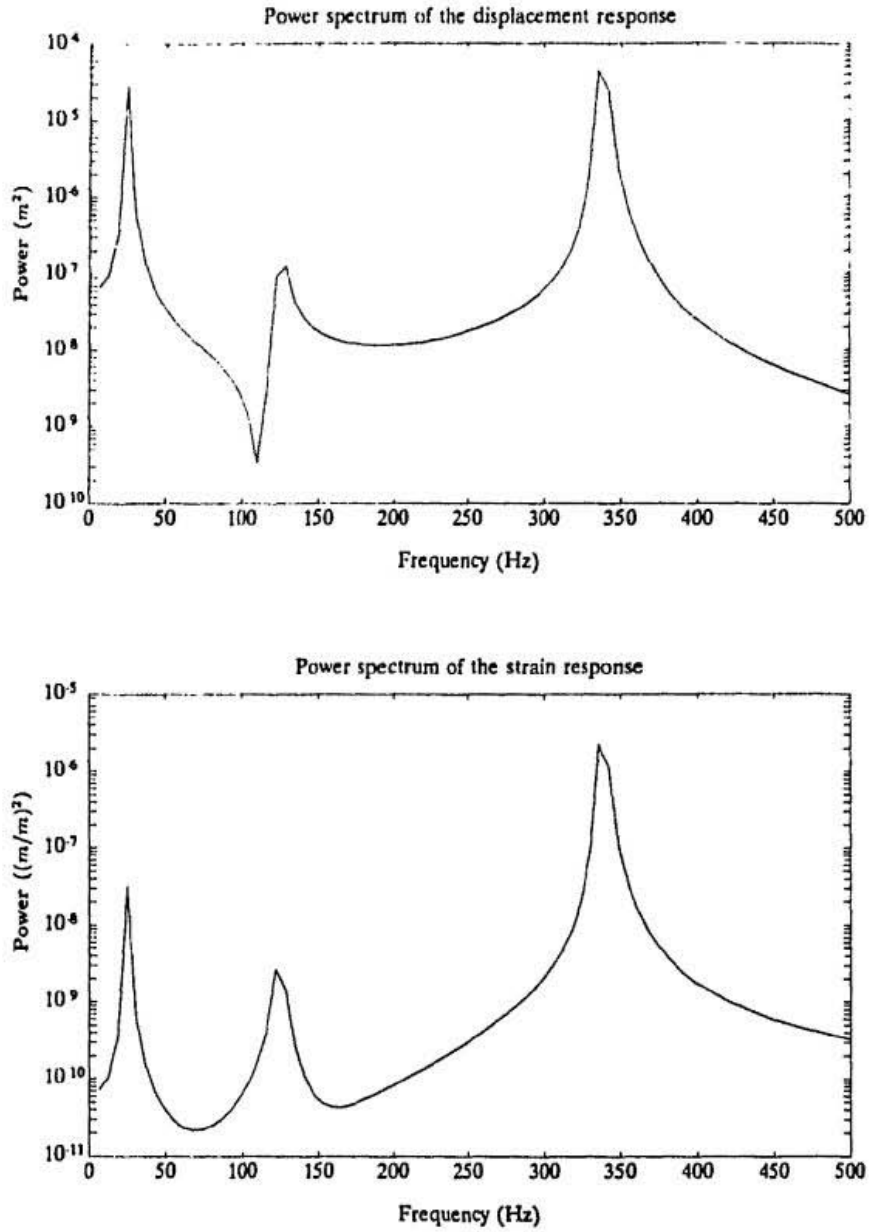

Figure 5.7: Power spectrum of the responses when excited at ω_3

the plate is excited at the third bending frequency.

As in the case of frequency response functions, the power spectrum of the strain response will also show a large decrease in the amplitude of peaks at resonant frequencies when there is a crack in the structure. The power spectrum of the displacement response shows very little change due to the crack. Figs. 5.8 and 5.9 show the change in power spectra of the strain and displacement responses due to the crack. Therefore the power spectrum of the local resonant strain response can also serve as an indicator of cracking occurring in the structure. It must be remembered that in this study, the excitation force amplitude is a fixed value and does not change throughout the whole duration of analysis. Since the response is directly related to the amplitude of excitation, different excitation forces will show varying values of structural responses. In real structures, the excitation (applied) forces generally varies from time to time. So it would be difficult to tell whether the changes in the power spectrum of the response is caused by changes in applied forces or caused by the presence of cracks. Therefore the practical usage of this method is limited.

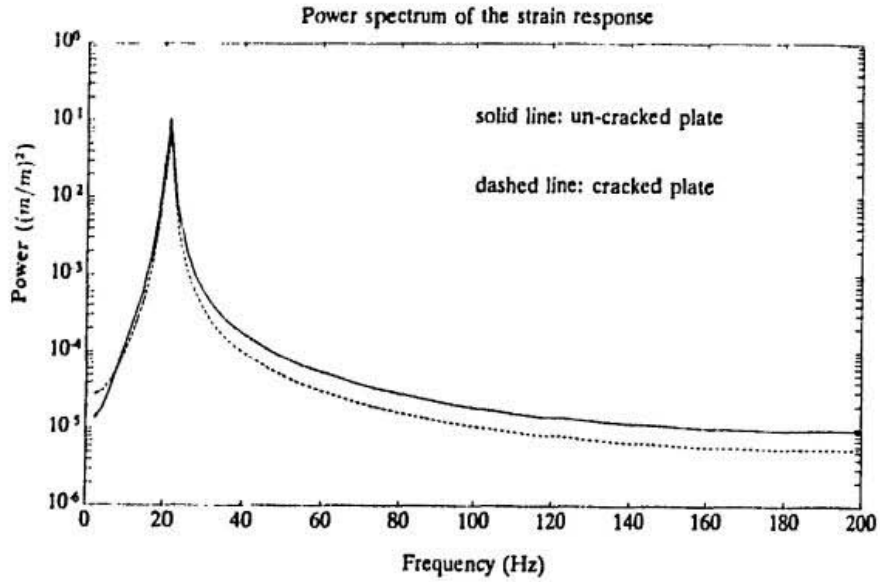

Figure 5.8: Power spectrum of the strain response, with/without the crack

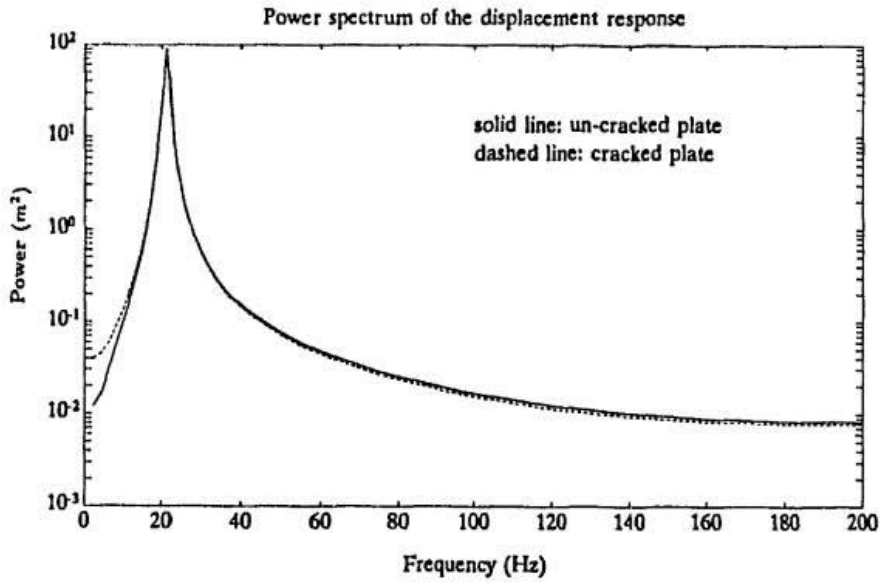

Figure 5.9: Power spectrum of the displacement response, with/without the crack

5.2 Strain Mode Shapes

5.2.1 Definition and Method of Extraction

The displacement mode shapes are obtained during the eigenvalue extraction process and are shown in chapter 4. Since the strain mode shape is a relatively new concept, the techniques for its calculation are not well developed in the general purpose computer software available in open market. ABAQUS does not have the option to do so. In this study, similar to the displacement mode shape, the strain mode shape is defined as the surface strain response of the structure when it vibrates at a certain resonant frequency; the surface strain values of the structure are normalized to a unit maximum value to obtain the strain mode shapes.

In this study, only the lowest bending modes are considered; so only the surface strain values along the centre line of the plate are required to be calculated to get the approximate bending strain mode shapes. Fig. 5.10 shows the three strain mode shapes corresponding to the first three bending modes.

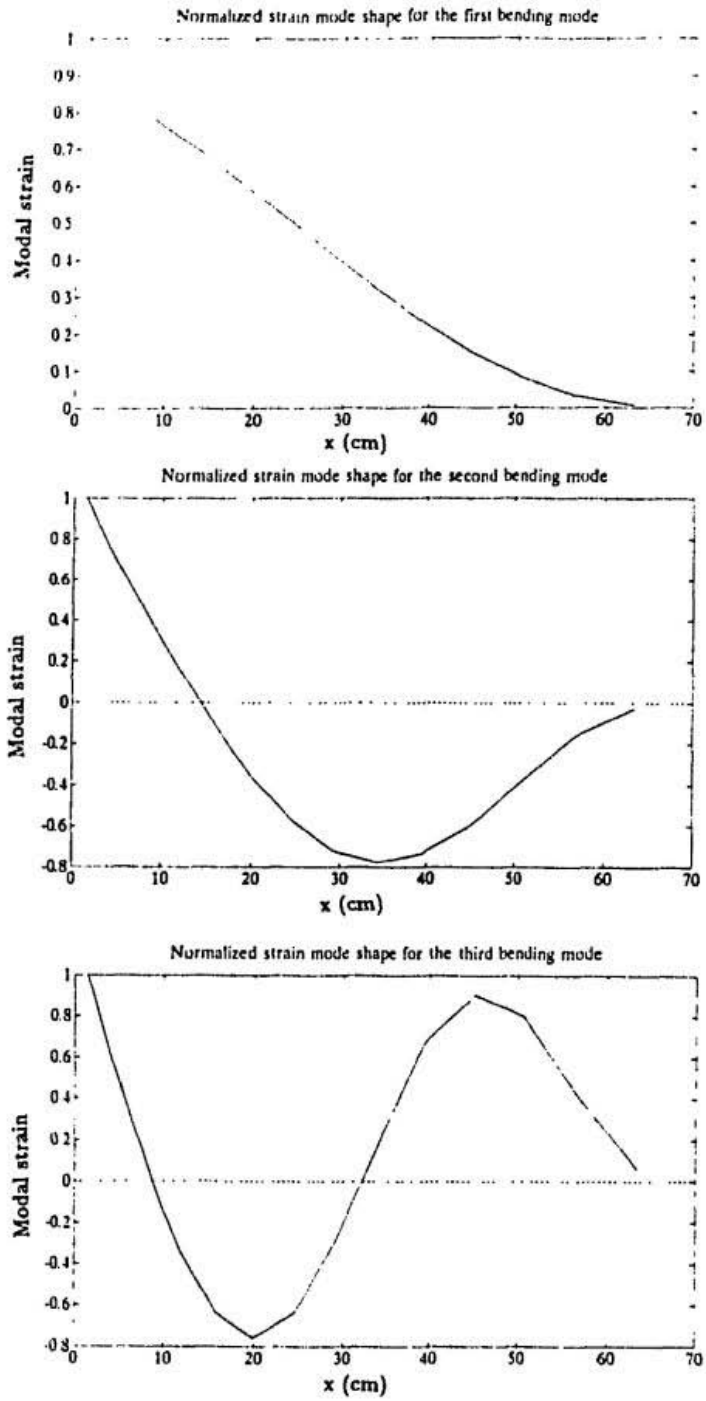

Figure 5.10: First three bending strain mode shapes

5.2.2 Strain Mode Shape Changes Due to the Growth of the Depth of the Crack

Since local strain values are very sensitive to the crack, strain mode shapes may also be very sensitive to the crack. Actually, it is shown to be one of the best method to find out the location and severity of the crack in the structure. Fig. 5.11 shows the strain mode shape changes for all the three bending modes as the depth of the crack grows . It is clear from these figures that around the crack there is a big drop in strain mode shape amplitudes for all the three modes. As the depth of the crack increases, the drop become larger. It is obvious that this change in strain mode shape can be used as a clear indicator of the location and severity of the crack in the structure.

All the strain mode shapes here are normalized with respect to the largest strain amplitude. We find that by plotting the differences of the normalized strain mode shapes, it is much easier to show the changes that occur, and to identify the location of the crack that occurs in the structure. Fig 5.12 gives the differences of the normalized strain mode shapes between the uncracked and cracked plate (for the first three bending frequencies). It is observed that for all the three modes, a large peak occurs at the position where the crack occurs. This peak can be used for detecting cracking in structures. The location of the

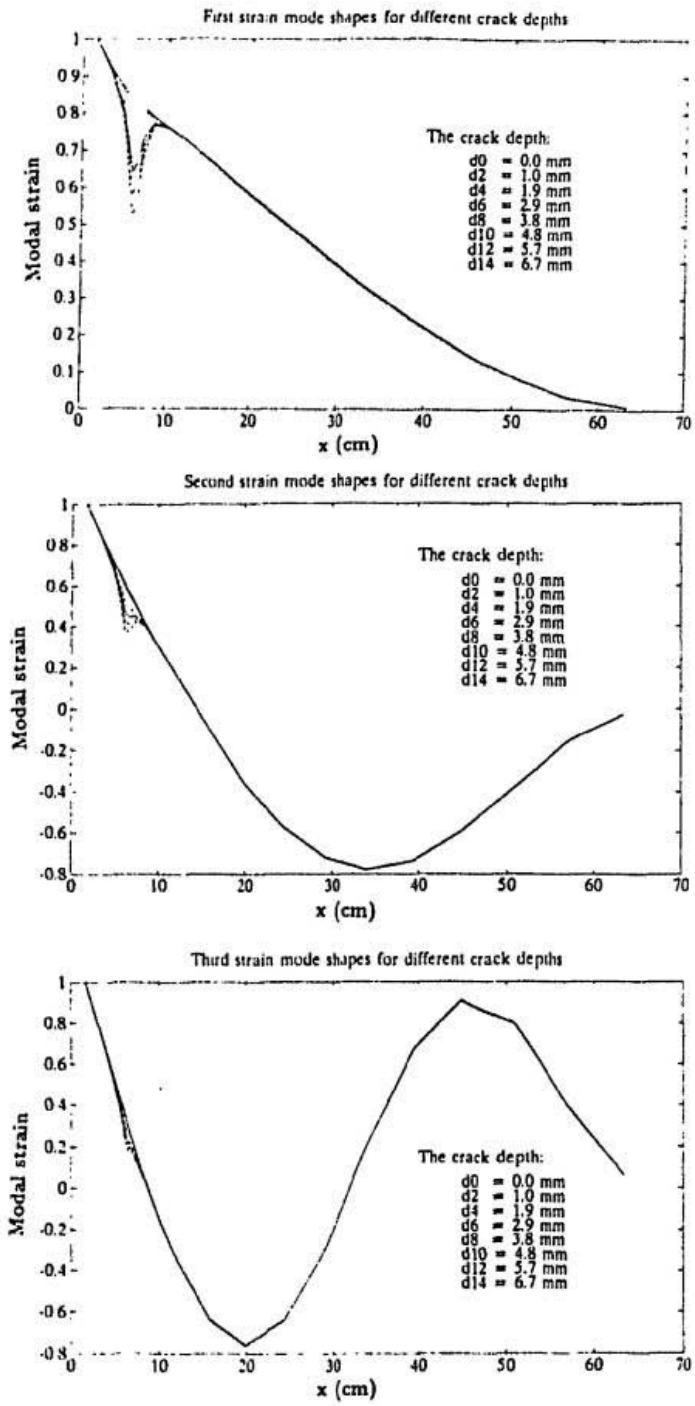

Figure 5.11: Strain mode shape changes due to increase in the depth of the crack

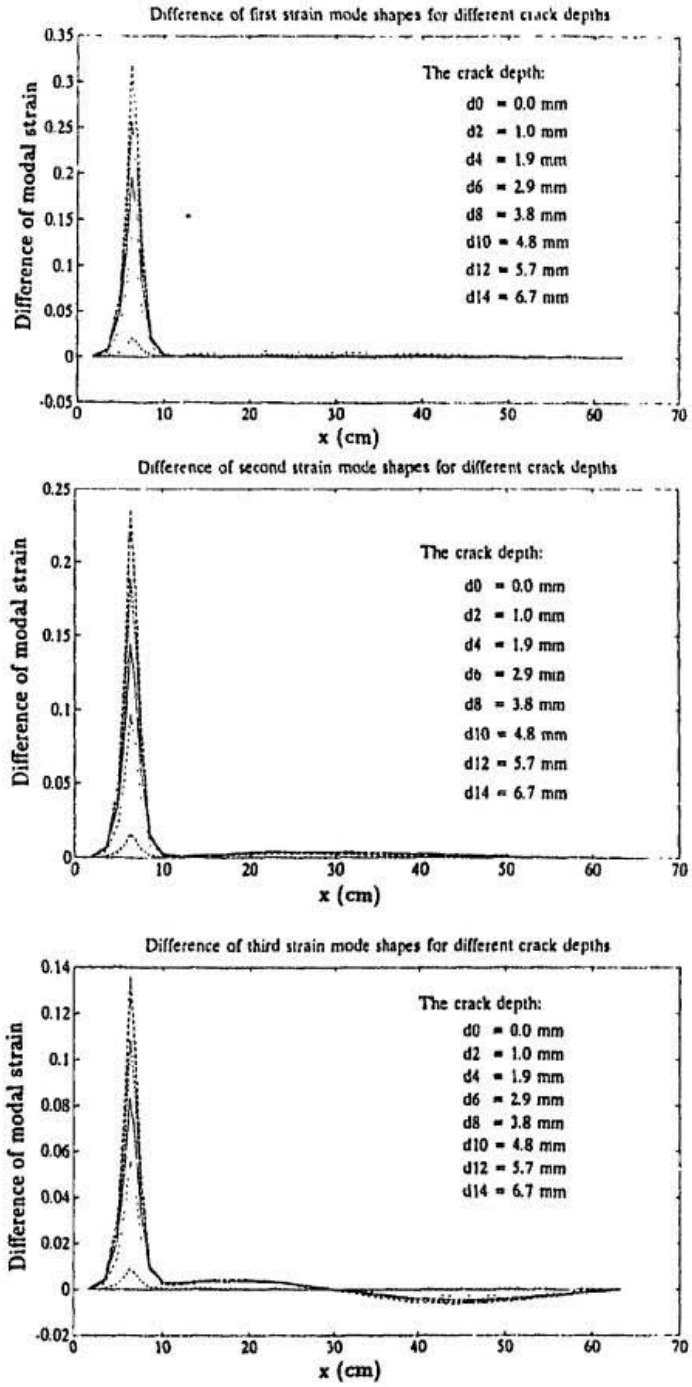

Figure 5.12: Differences of the strain mode shape for the first three bending modes

peak in the difference of the strain mode shapes indicates the position of the crack, and the amplitude of these peaks can be used to indicate the severity of the crack. A higher amplitude of the peak in the difference of the strain mode shape indicates a more severe crack that has occurred in the structure. For the same crack, different modes will have different amplitudes of the peak in the difference of the strain mode shape. If the crack is close to the nodal point of one mode, the amplitude of the peak corresponding to that mode will be small. From the strain mode shapes shown in Fig. 5.10, it is observed for the third bending mode that the crack is close to the nodal point. Therefore the changes in that strain mode shape are small around the crack in comparison to the other two modes (Fig. 5.11); the amplitude of the peak in the difference of the strain mode shape is also small(Fig. 5.12). Another important observation that can be made from Fig. 5.12 is that the modal strains undergo significant changes even at positions away from the crack. Hence strain gauges tend to be better indicators of cracking even at distances very far away from the crack.

The complete procedure for detecting cracks in the structure by monitoring of the difference of the strain mode shapes can be summarized as follows:

(a) Strain modal analysis is performed and normalized strain mode shapes are calculated and stored.

(b) After a crack has occurred in the structure, the first step is repeated once again.

(c) Compare the strain mode shapes obtained in steps 1 and 2. Find the difference and plot it. Thus the difference of the strain mode shapes is obtained.

(d) Find the peak in the difference of the strain mode shape. The location of the peak indicates the position of the crack, and the amplitude of the peak indicates the severity of the crack.

5.3 Impulse Excitation

5.3.1 Time History

An impulsive force is defined as a large force that acts for a very short duration of time. Mathematically, it can be expressed in terms of the delta function: $F = I\delta(t)$. In the numerical analysis, this "very short duration of time" has to be given. In our case, it is chosen to be 0.0006 sec. As in the case of sinusoidal excitation, this value is a compromise for considering the interested frequency range, the accuracy in describing the response, and limits in the computer disk space and the CPU time. The time history of the excitation force is shown in

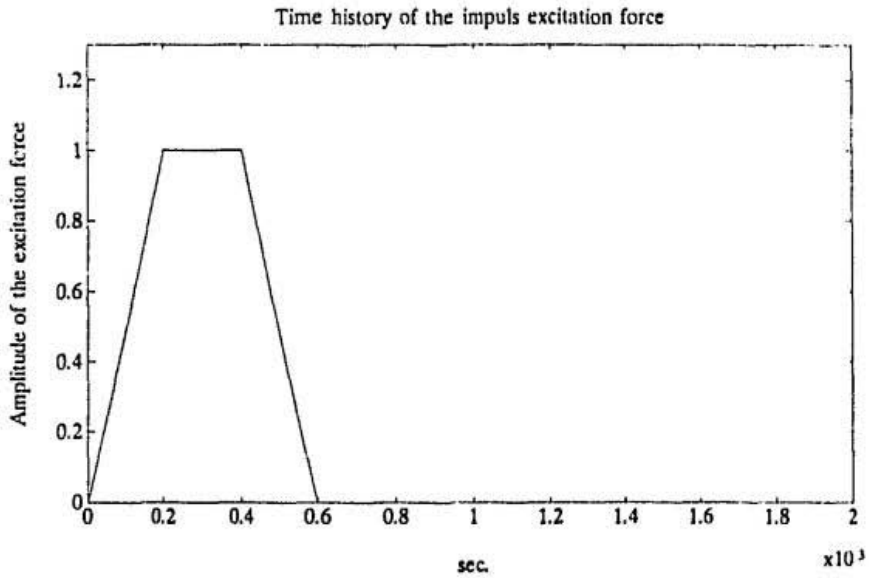

Figure 5.13: Time history of the excitation force

Fig. 5.13. The method and procedure for the calculation of the time history for the impulse excitation are similar to the ones for the sinusoidal excitation. The impulse excitation force is applied at the centre of the free end. When the structure is under the impulse excitation, the structure will have two types of responses; during the period of the impulse the structure will respond under the influence of the force; thereafter, the structure will vibrate freely with the defined boundary conditions and the imparted initial conditions at the ceasing of the impulsive force excitation. The responses will contain all the natural frequencies; and the fundamental frequencies will contain more power. In this case, the first three bending modes will be the major frequency components in

Table 5.1: Changes in the displacement and strain responses

time (sec)	0.0380	0.0952	0.1480
strain ($\mu\epsilon$) (7.8 mm away from the crack)			
uncracked	23.004	21.546	15.304
crack	18.435	17.240	12.879
change (%)	19.9	20.0	15.9
displacement (mm) (at the free end)			
uncracked	0.6099	0.4971	0.4603
cracked	0.6034	0.5123	0.4760
change (%)	1.1	-3.1	-3.4

the responses. Figs. 5.14 and 5.15 show the displacement response and strain response of the plate with and without the crack. The measurement point for the displacement response is at the free end of the plate. The measurement point for the strain response is at the centre line 7.8 mm away from the crack. Table 5.1 gives the displacement and strain responses at 0.038 sec, 0.095 sec, and 0.15 sec, for the uncracked and cracked plates.

Similar to the previous studies, the amplitude of the strain response for the cracked plate is smaller than for the uncracked plate, when the applied forces are the same, the changes are around 20.0%. The displacement response changes are very small for the cracked and uncracked plates.

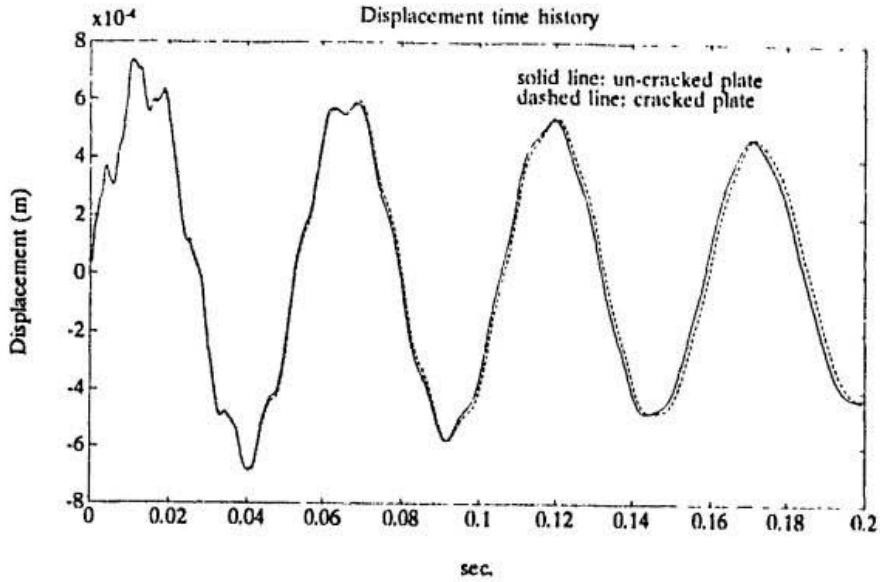

Figure 5.14: Displacement response under the impulse excitation

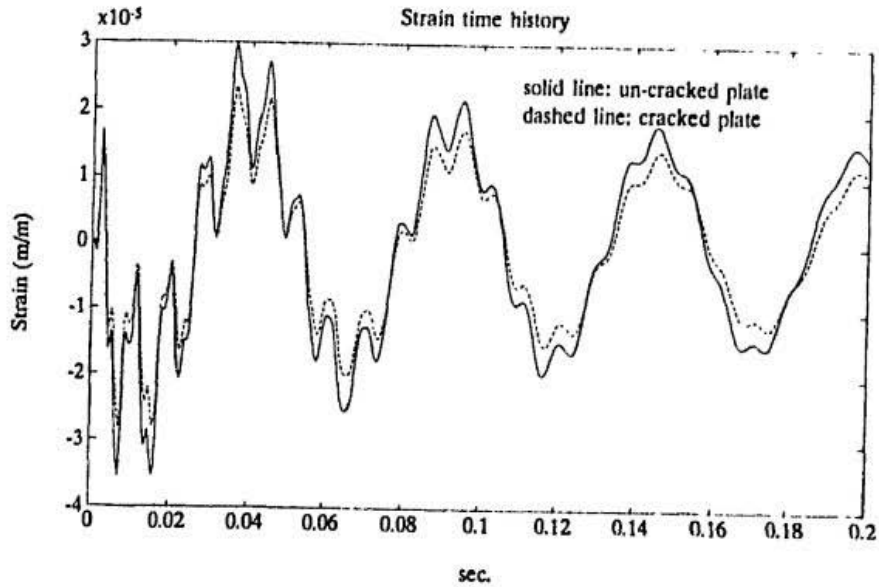

Figure 5.15: Strain response under the impulse excitation

5.3.2 Power Spectrum

Figs. 5.16 and 5.17 show the power spectra of Figs. 5.14 and 5.15, respectively. The frequency resolution for the power spectra is 5 Hz. The use of this coarse resolution is due to the limitation in the computer disk space and the CPU time. Although it will not give a very accurate estimation of the power spectrum, it will be enough for the understanding of the trend and the power distribution in the frequency domain.

From Figs. 5.16 and 5.17, it is observed that the first peak (corresponding to the first bending mode) is the largest; the second peak (corresponding to the second bending mode) is smaller than the first peak; and the third peak (corresponding to the third bending mode) is smaller than the second one. It indicates that the power utilized for the fundamental mode vibration is larger than that for the higher modes in the impulse excitation. It is also observed that there are significant decreases of the amplitudes in the power spectrum of the strain response when the crack is introduced; the power spectrum of the displacement response has almost insignificant changes. It is similar to the case of sinusoidal excitation and static behaviour. Again this method has its limitation in the practical usage because the power spectrum is only based on the response, and the responses would change when the amplitude

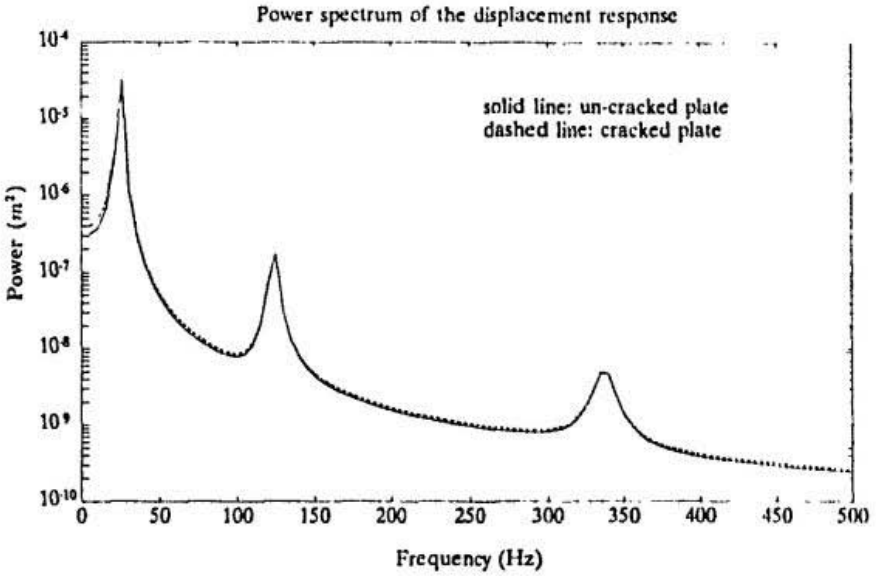

Figure 5.16: Power spectrum of the displacement response

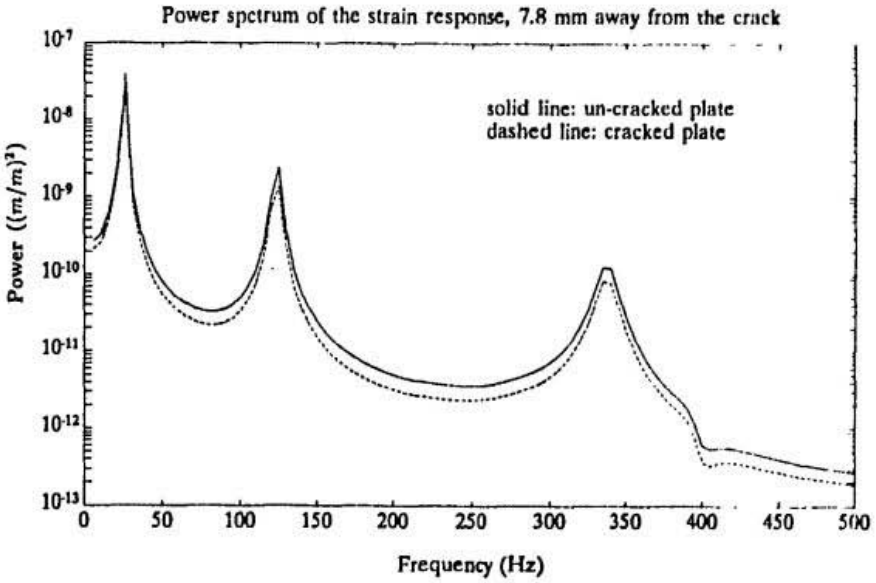

Figure 5.17: Power spectrum of the strain response

Table 5.2: Changes in amplitudes of the power spectrum of the strain response at nonresonant points. 7.8 away from the crack

Frequency (Hz)	80	245
uncracked	3.2367e-11	3.5943e-12
cracked	2.1755e-11	2.3190e-12
change (%)	32.79	35.8

of excitation is changed. Another important fact to be observed is that the strain levels decrease considerably for the cracked structure in the regions away from resonance as shown in Table 5.2. This could be used to advantage in the procedure using acoustic intensity methods for crack detection.

Chapter 6

Conclusion

When there is a surface crack in the plate the physical properties, as well as modal properties, of the plate change. From this study, we know that these changes in physical properties and modal properties are reflected in the stress/strain fields around the crack in static case; and in the shifts of natural frequencies, changes in the frequency response function and strain mode shapes in the dynamics cases. Further more, we find that local strain frequency response functions and strain mode shapes, as well as static strain level in these areas, are the most sensitive parameters to the crack occurring in the plate. Although the experimental set up for modal testing is more complicated than the static ones, it has the advantage that the modal parameters are indepen-

dent of the amplitude of the applied forces. Modal parameters are obtained when the structure is under resonant conditions. Therefore the applied force could be smaller than that in the static measurement, when good and reliable response outputs are obtained. In the areas which are not close to the crack, modal testing at high modes may give larger changes in the amplitude of the strain FRFs than changes from static measurements.

Based on this systematic study of the mechanical behaviour of the plate with a surface crack, the following conclusions can be made:

(a) Modal analysis which monitors the modal parameters such as natural frequencies, mode shapes, modal displacements and modal strains, can be used as an efficient technique for crack detection.

(b) Cracks in the structure will cause the reduction of the natural frequencies, which can be used as a global indicator of cracks occurring in the structure; but it must be used cautiously since these changes are very small.

(c) Performing the strain modal analysis and focusing on the local strain frequency response function, is a sensitive and practically useful method for detecting and localizing the surface cracks occurring in a structure.

(d) From the strain modal analysis, the strain mode shapes can be obtained.

By calculating the differences of the strain mode shapes and obtaining the location of the largest difference (peak), the location and the depth of the crack can be determined.

Although the study is only carried out for a rectangular plate, it is believed that the conclusions stated above can be extended to more complex structures. Therefore, it is believed that modal testing can be used for crack detection in real structures. First the natural frequencies should be monitored. This can be done by performing the modal testing with accelerometers or strain gauges which have been located at any convenient position of the structure. If there is a reduction in natural frequencies, cracks could have occurred in the structure (as mentioned earlier in Chapter 1, other causes such as soil erosion around the base of the structure, strength degradation of the foundation soil, marine fouling, incidental weight increases in the platform deck weight, etc., will also cause a shift in the frequency to occur; these causes must be eliminated before using this procedure for crack detection).

For more accurate detection of the crack, it is suggested that strain gauges be attached to several critical reference points where the structural behaviour can be represented from earlier numerical analysis. Then the strain modal testing should be performed and difference of the strain mode shapes, as stated

above be calculated. Locating the largest difference between the modal strain response the position of the crack can be determined.

For more complex structures, it would be difficult to attach strain gauges all along the structure to get the strain mode shapes. In this case, it is suggested that the strain gauges be located in the critical areas. The strain modal testing should be performed and the local strain frequency response functions obtained. Find the largest drop in the amplitude of the strain frequency response function, and the location of the crack is determined to be located near the corresponding strain gauge.

In order to get the strain frequency response function and strain mode shapes, the excitation force has to be measured. For the case of single excitation, it is easy to attach a force transducer to record to the excitation force. For real structures, in many cases the forces are applied all along the structure and are continuously distributed. For example, in offshore platforms, the forces are distributed along the depth of the structure under water. In these cases, multiple input output techniques may be needed to get the frequency response function in the proper simulation for modal analysis. More studies are needed in these areas in the future.

Damping of the structure under the dynamic excitation is also a very impor-

tant parameter in the determination of the structural response. This study did not address the change in damping as the crack depth grows. If the relationship between the damping and crack depth and/or location could be derived theoretically or experimentally, it could also be used in the detection of cracks in the structure. Therefore, examination the damping changes in a cracking structure could also be investigated in future studies.

References

Bernasconi, O. and Ewins, D.J., 1989. "Modal Strain/Stress Fields ", The International Journal of Analytical and Experimental Modal Analysis, Vol.4, No.2, April, pp. 68-76.

Bernasconi, O. and Ewins, D.J., 1989. "Application of Strain Modal Testing to Real Structures", Proceedings of the VIIth International Modal Analysis Conference, U.S.A., Vol. II, pp. 1453-1464.

Chen, Y. and Swamidas, A.S.J., 1992. "Modal Changes to Crack Growth in a Tripod Tower Platform", accepted for publication in the Canadian Journal of Civil Engineering, October.

Chondros, T.G. and Dimarogonas, A.D., 1980. "Identification of Cracks in Welded Joints of Complex Structures", Journal of Sound and Vibration, Vol. 69(4), pp. 531-538.

Chondros, T.G. and Dimarogonas, A.D., 1989. "Dynamic Sensitivity of Structures to Cracks", Journal of Vibration, Acoustics, Stress, and Reliability in Design, Vol. 111, pp. 251-256.

Collins, K.R., Plaut, R.H., and Wauer, J., 1991. "Detection of Cracks in Rotating Timoshenko Shafts Using Axial Impulses", Journal of Vibration and Acoustics, Vol. 113, pp. 74-78.

Collins, K.R., Plaut, R.H., and Wauer, J., 1992. "Free and Forced Longitudinal Vibrations of a Cantilevered Bar with a Crack", Journal of Vibration and Acoustics, Vol. 114, pp. 171-177.

Ewins, D.J., 1984. "Modal Testing: Theory and Practice", J.Wiley Inc., Research Studies Press Ltd.

Gomes, A.J.M.A. and Silva, J.M.M., 1991. "Theoretical and Experimental Data on Crack Depth Effects in the Dynamic Behaviour of Free-free Beams", Proceedings of the IXth International Modal Analysis Conference, Italy, April, Vol. I, pp. 274-283.

Gomes, A.J.M.A. and Silva, J.M.M., 1990. "On the Use of Modal Analysis for Crack Identification", Proceedings of the VIIIth International Modal

Analysis Conference, Florida, U.S.A., Vol. II, pp. 1108-1115.

Guigne, J.Y., Klein, K., Swamidas, A.S.J., and Guzzwell, J., 1992. "Modal Information from Acoustic Measurements for Fatigue Crack Detection Applications", Proceedings of the 11th International Conference on Offshore Mechanics and Arctic Engineering, Vol.I, Part B, pp. 585-594.

Hearn, G. and Testa, R.B., 1991. "Modal Analysis for Damage Detection in Structures", Journal of Structural Engineering, Vol. 117, No. 10, Oct., pp. 3042-3063.

Hibbitt, Karlsson & Sorensen, Inc., 1989. "ABAQUS, Example Problems Manual", Version 4.8.

Hibbitt, Karlsson & Sorensen, Inc., 1989. "ABAQUS, Theory Manual", Version 4.8.

Hibbitt, Karlsson & Sorensen, Inc., 1989. "ABAQUS, User's Manual", Version 4.8.

Ilanko, S. and Dickinison, S.M., 1991. "On Natural Frequencies of Geometrically Imperfect, Simply-Supported Rectangular Plates Under Uniaxial Compressive Loading", Journal of Applied Mechanics, Vol. 58, Dec., pp. 1082-1084.

Li, D., Zhuge, H., and Wang, B., 1989. "The Principle and Techniques of Experimental Strain Modal Analysis", Proceedings of VIIth International Modal Analysis Conference, U.S.A., Vol. II, pp. 1285-1289.

Li, D., Zheng, Z., He, K., and Wang, B., 1992. "Damage Detection in Offshore Structures by the FRF Method", Proceedings of the XIth International Conference on Offshore Mechanics and Arctic Engineering, Calgary, Canada, Vol.I, Part B, pp. 601-604.

Parks, D.M., and White, S.C., 1982. "Elastic-Plastic Line Spring Finite Elements for Surface Cracked Plates and Shells", Journal of Pressure Vessel Technology, Vol. 104, pp. 287-192.

Pandy, A.K., Biswas, M., and Samman, M.M., 1991. "Damage Detection from Changes in Curvature Mode Shapes", Journal of Sound and Vibration, Vol.145 (2), pp. 321-332.

Rajab, M.D. and Al-Sabeeh, A., 1991. "Vibrational Characteristics of Cracked Shafts", Journal of Sound and Vibration, Vol. 147(3), pp. 465-473.

Rice, J.R., 1972. "The Line Spring Model for Surface Flaws", The Surface Crack: Physical Problems and Computational Solutions, J.L. Sedlow, Editor, ASME.

Richardson, M.H., and Mannan, M.A., 1991. "Determination of Modal Sensitivity Functions for Location of Structural Faults", Proceedings of the IXth International Modal Analysis Conference, Italy, Vol. I, pp. 670-676.

Rogers, L.M., Monk, R.G., 1987. " Detection and Monitoring of Cracks in Offshore Structures", presented at the 19th Annual Offshore Technology Conference in Houston, Texas, USA.

Sanliturk, K.Y., and Imregun, M., 1990. "Theoretical Modelling of the Damping Produced by Fatigue Crack", Proceedings of VIII International Modal Analysis Conference, Vol. II, pp. 1370-1374.

Shahrivar, F. and Bouwkamp, J.G., 1986. "Damage Detection in Offshore Platform Using Vibration Information", Journal of Energy Resources Technology, Transaction of the ASME, June, Vol. 108, pp. 97-106.

Silva, J.M.M., and Gomes, A.J.A., 1992. "On the Use of Modal Analysis for Fatigue Crack Detection in Simple Structural Elements", Proceedings of the XIth International Conference on Offshore Mechanics and Arctic Engineering, Calgary, Canada, Vol. I, Part B, pp. 595-600.

Springer, W.T., Stuff, S.A., Coleman, A.D., and Driskell, T.A., 1991. "Simulating the Presence of Damage in a Vibrating Structure with Finite Element and Structural Dynamics Modification Techniques", Proceedings of the IXth International Modal Analysis Conference, Italy, Vol. II, pp. 1108-1109.

Stubbs, N., and Osegueda, R., 1990. "Global Non-Destructive Damage Evaluation in Solids", The International Journal of Analytical and Experimental Modal Analysis, 1990 Apr., pp. 67-79.

Swamidas, A.S.J. and Chen, Y., 1992. "Damage Detection in a Tripod Tower Platform (TTP) Using Modal Analysis", Proceedings of the XIth International Conference on Offshore Mechanics and Arctic Engineering, Calgary, Canada, Vol. I, Part B, pp. 577-583.

Tsang, W.F., 1990. "Use of Dynamic Strain Measurements for Modelling of Structures", Proceedings of the VIIIth International Modal Analysis Conference, U.S.A., Vol. II, pp. 1246-1251.

Zienkiewicz, O.C. and Taylor, R.L., 1989. "The Finite Element Method", McGraw-Hill Book Company.